JOURNAL OF NUCLEAR MATERIALS 26 (1968) 18–50. © NORTH-HOLLAND PUBLISHING CO., AMSTERDAM

MECHANISMS FOR THE IN-REACTOR CREEP OF ZIRCONIUM ALLOYS

G. R. PIERCY

Chalk River Nuclear Laboratories, Atomic Energy of Canada Ltd., Ontario, Canada

Received 18 September 1967

Qualitative estimates are made for the various factors that may influence the creep rate of zirconium alloys during reactor irradiation. Comparison of these with experimental measurements indicates that the in-reactor creep rate of cold-worked Zircaloy is due to dislocation climb caused by the supersaturation of vacancies and interstitials that is introduced by irradiation. The effect of an internal stress distribution introduced by radiation growth does not appear to be an important creep mechanism in cold-worked Zircaloy.

Des estimations qualitatives ont été faites de la valeur des divers facteurs qui peuvent influencer la vitesse de fluage des alliages de zirconium durant l'irradiation dans un réacteur. La comparaison de ces valeurs avec les mesures expérimentales indique que la vitesse de fluage en réacteur du Zircaloy écroui à froid est due à la montée des dislocations causée par la sursaturation des lacunes et des interstitiels introduits par l'irradiation.

L'effet d'une distribution de tensions internes introduites par la croissance sous irradiation ne semble pas être un mécanisme important pour le fluage dans le Zirconium écroui à froid.

Es werden qualitative Abschätzungen angegeben für verschiedene Faktoren, die die Kriechgeschwindigkeit von Zirkonium-Legierungen während Reaktor-Bestrahlung beeinflussen können. Der Vergleich mit Messergebnissen deutet darauf hin, dass die Kriechgeschwindigkeit beim kaltbearbeiteten Zirkaloy von der Zunahme von Versetzungen herrührt, die durch Übersättigung von Leerstellen und Zwischenatomen (entstanden durch Bestrahlung) herrührt. Der Effekt einer Verteilung innerer Spannungen aufgrund der Bestrahlung scheint keine Bedeutung für den Kriechmechanismus zu haben.

1. Introduction

The effect of irradiation on the creep rate of zirconium alloys is of particular importance in the design of pressure tube reactors. Chockie et al. [1]), who measured the in-reactor creep rate of cold worked Zircaloy up to a few hundred hours at relatively high stresses or temperature, reported a small reduction in creep rate caused by irradiation. Fidleris and Williams [2]) have used a more sensitive apparatus to measure the creep rate of cold worked Zircaloy under a stress of 20 kpsi (14.1 kg/mm^2) at 300 °C. After three thousand hours the creep rate measured inside the reactor was ten times the rate measured outside the reactor. They also gave a comprehensive review of related experiments and theoretical models of in-reactor creep.

The purpose of this paper is to examine the most promising of these models by estimating their various parameters. The qualitative experimental features that need explaining are:

1. The in-reactor creep rate of cold-worked Zircaloy reaches a relatively constant value after several hundred hours irradiation [2, 3]);
2. The magnitude of the constant in-reactor creep rate of cold-worked Zircaloy increases with temperature in the region 200–350 °C and with stress in the region 10–30 kpsi (7–21 kg/mm^2) [4]);
3. When the reactor is shut down the creep rate of cold-worked Zircaloy decreases to a value near that of the comparable out-reactor test within about one hundred hours [2]);

4. If the cold-worked Zircaloy has been pre-crept at the same stress outside the reactor, the higher in-reactor creep rate begins immediately the irradiation begins. There is no appreciable incubation period [2]);
5. Pre-irradiation of cold-worked Zircaloy does not affect the in-reactor creep curve using a stress of 20 kpsi (14.1 kg/mm^2) at 300 °C [4]);
6. The constant in-reactor creep rate of heat treated Zr-2.5 wt % Nb is usually initially below that of the out-reactor rate and remains so until the out-reactor rate decreases to a lower value [3, 4]). The in-reactor rate is also below the out-reactor rate in cold-worked Zircaloy when the stress is 45 kpsi (31.7 kg/mm^2) [4]).

Irradiation can increase the creep rate by mechanisms involving the formation of dislocation loops, mobile point defects or an increased dislocation density. It can decrease the creep rate by introducing regions of radiation damage, including loops, as obstacles to dislocation motion. These several possibilities will be treated in turn. As a necessary background, Appendix A summarizes the present state of knowledge of radiation damage and point defects in zirconium.

2. Increase in creep rate caused by the formation of dislocation loops

Dislocation loops are thought to be caused by the collapse of vacancy or interstitial aggregates onto specific lattice planes. This introduces a local strain perpendicular to the plane, which gives a direct contribution to the creep rate if the orientation of the planes are not randomly distributed with respect to the stress axis. Two examples of this are given below. Another contribution to the creep rate is also considered, which arises from the internal stress introduced when the strain due to loop formation is anisotropic in each grain.

If all the loops in one grain are naturally aligned on parallel planes there will be a net strain, called radiation growth, in that grain. The component of this strain parallel to the stress axis will contribute directly to the creep of a single crystal. There will be a corresponding direct contribution to the creep of a textured polycrystal. The preference for loops to form on a specific type of lattice plane may be caused by a different stacking fault energy, elastic modulus, or local stress on these planes. Buckley [5]) discusses several of the factors that may cause this. It seems unlikely that the local stress caused by anisotropic expansion within the temperature spike is the dominant reason, however. The calculations in Appendices B and C indicate that the contribution of this stress is small compared with the other energy terms in the formation of these dislocation loops. Appendix B gives estimates of internal stress and appendix C of dislocation loop energy.

A similar direct contribution to the in-reactor creep rate results if the applied stress causes the dislocation loops to form on parallel planes, even though they may not normally do so [6]). The calculations in appendix C show that an applied stress is unlikely to change the type of crystallographic plane on which the loops form. However, it could still cause the loops to form on those planes of the preferred type that are at an optimum orientation relative to the direction of the applied stress, and may be effective even in random polycrystals if there are several planes of this type in each grain.

The direct change in sample dimensions is the only effect of radiation growth that is expected for a single crystal. The growth is always accommodated by a change in sample dimensions. In polycrystals, however, the constraint of neighbouring grains will prevent this change in dimensions. An elastic stress will build up which produces an elastic strain equal in magnitude but opposite in direction to the growth strain. The rate of increase of this internal stress during irradiation of zirconium is calculated in appendix B to be a tensile stress of 2.7 psi (1.9 g/mm^2) per hour perpendicular to the basal plane and a hydrostatic compression of 0.81 psi (0.57 g/mm^2) per hour, if the fast neutron flux is 1×10^{13} n/cm^2·sec, and the

radiation growth coefficient perpendicular to the basal plane is $G = -1$ per neutron. If there is no external stress this elastic stress will reach a limiting value when it is sufficiently high to cause a plastic creep rate that is equal in magnitude but opposite in direction (crystallographically) to the growth rate. If there is an external stress, the internal stress will build up until the creep rate of individual grains is equal to their growth rate plus the average creep rate. This creep rate within the grains that relaxes the internal stress during irradiation will be called the "basic" creep rate. Because this basic creep which accommodates the growth strain is occurring during irradiation, an enhancement of the creep rate caused by any other mechanism may reduce the limiting value of this internal stress. This whole subject of internal stress is most clearly seen by using the nut-and-bolt analogy which is applied to this case in appendix D.

The effect of this internal stress distribution on the macroscopic creep rate of a polycrystal is difficult to calculate accurately. Blackburn indicated one method, which assumed the same total strain in all grains [7]). His alternate calculation, which was more completely developed because of its relative simplicity, averaged the creep rate over all the grains, ignoring their interaction. Further references to his work will be to this second calculation [7]). While this second assumption appears worse than the first, it has been used successfully to estimate the texture dependence of thermal expansion and growth in polycrystals [8, 9]). In addition Blackburn also assumed that the maximum value of the internal stress was independent of the applied stress, which is contrary to what one expects from examination of the nut-and-bolt analogy of appendix D. An estimate of the maximum internal stress is extremely important as it is one of the critical parameters that determine the long-term creep properties of reactor pressure tubes, if internal stress is the cause of the higher in-reactor creep rate. This final assumption was examined using a slightly simpler model than Blackburn's. Appendix E gives a calculation which averages the creep rate of the grains using a one-dimensional model in place of Blackburn's three-dimensional case which used the deviator stress. The difference between the two calculated creep enhancements was not significant for these arguments and was mainly due to the simpler stress distribution assumed in the one-dimensional model. The model was then used to estimate the effect of the applied stress on the maximum value of the internal stress achieved during irradiation. The effect of the applied stress was very great at the stress levels required to explain the large creep rate enhancement measured in Fidleris's in-reactor tests on cold-worked Zircaloy. Until Blackburn's theory is corrected for this effect, the calculated values of maximum internal stress and hence maximum in-reactor creep rate will be too high.

The enhancement of the creep rate caused by an internal stress distribution is very dependent on the stress dependence of the basic creep rate which relaxes the internal stress. If the basic creep rate is proportional to $(\text{stress})^n$, then a value of n greater than 4 is probably required to explain the in-reactor creep rate of Zircaloy. Blackburn assumes the basic creep rate equals the out-reactor value, but for Zircaloy at 20 kpsi (14.1 kg/mm^2) this only has a value of n in the neighbourhood of two [10]). As discussed above, the basic creep rate during irradiation involves several unknown factors. However, assuming $n = 5$ and that the in-reactor creep rate is enhanced by the internal stress, the value of the radiation growth rate that is required to explain the measured creep rate can be calculated. Fidleris's test R6 had a creep rate enhancement of 8 between the value when the reactor was on and when it was off [2]). Using Blackburn's equation, as given in Hesketh's fig. 3 [11]), this requires an internal stress of 24 kpsi (17 kg/mm^2) if the applied stress is 30 kpsi (21 kg/mm^2). Since the integrated fast neutron flux was 2.2×10^{19} n/cm^2 at this point, the growth constant using the parameters of appendix B is $G = -14.6$ per neutron. This estimate is probably low in magnitude as there

was assumed to be no relaxation by plastic creep, the high value of $n=5$ was used, and the stress calculated in appendix B is an upper limit due to the chosen boundary conditions.

In many experiments the internal stress is not continually renewed but is relaxed with strain because the more highly stressed grains creep more rapidly than the average. Thus, the creep rate enhancement caused by the internal stress will decrease with plastic strain of the sample. The one-dimensional model was used to estimate how rapidly the creep rate enhancement decreased with strain when the internal stress was not being continually renewed. The calculation in appendix E shows that a creep strain similar to the elastic strain produced by the internal stress is required to reduce the creep rate enhancement to a low value. This is applicable to two types of experiment performed by Fidleris. The first type measures the change in creep rate when the reactor is shut down but the sample is maintained at the same stress and temperature. His test R6 showed a reduction in creep rate by a factor of seven within approximately one hundred hours after shut-down [2]). This corresponds to a creep strain less than 3×10^{-5}, which is less than two percent of the elastic strain introduced by an internal stress of 20 kpsi (14.1 kg/mm^2). An internal stress of this magnitude is required to explain the enhancement of creep rate by the factor of seven observed during irradiation. Thus a sufficiently high internal stress required to explain the enhancement of creep rate during irradiation is incompatible with the rapid drop in creep rate when the reactor is shut down.

The second type of experiment involving the relaxation of an internal stress is the effect on the in-reactor creep of a prior irradiation at the same temperature. Fidleris measured the in-reactor creep rate after an irradiation with 3×10^{20} fast n/cm^2. Assuming an internal stress of 20 kpsi (14.1 kg/mm^2) was introduced by this irradiation, the average creep rate enhancement up to a plastic creep strain of 0.08% should be equal to five, as calculated in appendix E. Thus, the pre-irradiated sample should creep to this strain in one-fifth the time of the sample not pre-irradiated. Fidleris's sample Rx-14, that received this prior irradiation, reached 0.08% plastic strain in the same time (within the experimental error of less than ten percent) as was required by sample R6, which did not receive a prior irradiation [4]). Thus, the mechanism of in-reactor creep involving an internal stress distribution does not appear to explain this experiment.

This increase in creep rate due to the internal stress is the only contribution of radiation growth to the in-reactor creep rate of randomly oriented polycrystals. There is no over-all change in sample dimensions with zero applied stress because the net internal stress and strain are zero in all directions. However, in a sample with a preferred texture this is no longer true. There will be a net growth strain in one direction which will relax the internal stress for grains aligned in the preferred direction but increase that of grains aligned in other than the preferred direction. The component of this net strain in the direction of the applied stress will be a direct contribution to the creep rate as for a single crystal. The stress relaxation results in a lower rate of increase of these internal stresses but the saturation value is probably still similar.

There is another way in which the creation of dislocation loops or other types of damage region can increase the creep rate. In some alloys dislocation mobility has been reduced by the segregation of solute atoms to the dislocations. If these solute atoms have a lower energy when associated with a region of radiation damage than when associated with a dislocation, as is thought to occur for nitrogen in iron [12]), then they will leave the dislocations during irradiation at 300 °C, thus increasing dislocation mobility. Current tests in progress at the Chalk River Nuclear Laboratories on the in-reactor creep rate of pure zirconium and Zircaloy in the annealed and cold-worked states are designed to check this mechanism but the possibility of strain-aging even in the "pure" zirconium may prevent any positive conclusion.

Appendix G gives a summary of the possible effectiveness of various solutes on the creep rate of Zircaloy. The calculations indicate that the normal amount of dissolved hydrogen, iron, chromium and nitrogen should not affect the creep rate unless they precipitate on dislocations. Oxygen, tin and niobium may have an effect.

3. Increase in creep rate caused by the formation of mobile point defects

Both interstitials and vacancies are probably mobile in Zircaloy at 300 °C (appendix A). These can cause climb of edge dislocations if they are annihilated at the jogs, which will produce a limited creep strain if the dislocations cannot slip [13]). Hesketh [14]) has considered this for the special dislocation array present in graphite. A similar phenomenon may also occur in other materials whose edge dislocations have their slip vector parallel to the tensile stress. However, a more general case is one in which the climb of the edge dislocations or of edge jogs in screw dislocations allows the dislocations to slip. A detailed estimate of this effect is given in appendix F. It is shown that the velocity of jogs causing climb in edge dislocations or the slower moving jogs that may limit slip in screw dislocations, is proportional to the fast neutron flux and to the difference between the concentration of sinks for interstitials and vacancies. If all the 10^{10} dislocations/cm^2 that are present in Fidleris's cold-worked Zircaloy samples are mobile, then a difference between the interstitial and vacancy sink concentrations of less than one part in a thousand would explain the in-reactor creep rate. Such a low value is expected if most of the interstitials are annihilated at radiation-induced vacancies. The calculation also indicates that the velocity of the jogs during irradiation is independent of the applied stress and the temperature. Thus, if climb is the rate-limiting mechanism, the effect of temperature and stress must arise through the terms involving the mobile dislocation density and the relative sink concentrations. Unfortunately, both of these are difficult to estimate with any certainty for an impure material in which dislocations and point defects may be held at many different impurities. However, if climb is the limiting mechanism, increasing the number of impurities that trap vacancies at 300 °C, should increase the fraction of interstitials that is annihilated at vacancies, thus reducing the in-reactor creep rate.

Another way in which the mobile vacancies and interstitials can increase the creep rate is by diffusing to the obstacles that impede the dislocation movement. If this reduces the interaction between the obstacle and the dislocation, then the dislocation will move more readily. An example of this would be the diffusion of interstitials to a dislocation loop which was produced by the condensation of vacancies. This could well be the case when regions of radiation damage are the obstacles, as seems likely in cold-worked Zircaloy at high stress and in heat treated Zr-2.5 wt % Nb, for reasons discussed later in section 5.

One of the few tools available with which to examine the detailed mechanism of any deformation process is the measurement of the activation energy and volume which controls the rate of deformation. These are discussed more completely in appendix H for the case of in-reactor creep. Holmes used the slope-change method (change in creep rate caused by a change in temperature) to measure an activation energy of 90 kcal/mole in Zircaloy when the reactor was on, compared to 60 kcal/mole when it was off [15]). The higher value with the reactor on is probably caused by a creep rate enhancement due to the supersaturation of defects that is induced when the temperature is raised. The creep rate can be increased either by the rapid thermal removal of radiation damage regions as obstacles to dislocations or by the removal of the excess point defects that are caused directly by the temperature rise or indirectly, by decomposition of the damage regions which have become unstable due to the temperature rise. It seems unlikely that it is the removal of the damage regions in their role as obstacles

to dislocation movement since the creep rate of cold-worked Zircaloy below 30 000 psi is not appreciably affected by prior irradiation. This leaves the model in which annihilation of excess point defects at dislocations is increasing the dislocation mobility.

Holmes et al. also measured the activation energy for the in-reactor creep in cold-worked Zircaloy by comparing the temperature dependence at constant stress, but the result is rather uncertain due to the scatter in experimental readings. Fidleris's results below 350 °C that are shown in appendix H give an activation energy of 21 kcal/mole at a tensile stress of 20 kpsi (14.1 kg/mm^2) and 8.4 kcal/mole at 30 kpsi (21 kg/mm^2). His results on the stress dependency at 300 °C indicate an activation volume less than $10b^3$ for the in-reactor creep, where b is the interatomic distance.

There is also the possibility that the brief temperature rise produced when a fast neutron collides with a nucleus will produce a stress pulse that is sufficient to move near-by dislocations, provided their momentum is sufficiently low. However, one would then predict an instantaneous change in creep rate when the reactor stopped, which is not observed.

4. Introduction of new slip dislocations by irradiation

It has been shown by electron microscopy that a long irradiation produces a large number of dislocation loops which interact to produce irregular dislocations [16]). If some of these dislocations can slip they will contribute to the creep rate. The calculation of dislocation loop energies given in appendix C indicates the perfect loop of lowest energy caused by vacancy condensation is on the $\{11\bar{2}0\}$ plane. The dislocation on one side of this loop is the normal slip dislocation for an adjacent $\{10\bar{1}0\}$ plane. Thus, it could act as a slip source if the loop or the stress was large enough. The contribution of these extra slip sources may be of particular importance for cases in which the creation of dislocations is difficult, as for a structure where the slip plane area is restricted by very fine precipitates or perhaps twins. In this case dislocations created at the grain boundaries cannot move very far into the grain, which makes dislocation sources inside the grain of more importance. This is probably not the mechanism for integrated fluxes up to 3×10^{20} fast n/cm^2 in Zircaloy or heat treated Zr-2.5 wt % Nb at 300 °C, however; Williams has observed only small isolated loops and black spots at this flux level [2]). However, it could be important at higher temperatures where larger loops are produced.

5. Decreased mobility of dislocations by irradiation

Regions of radiation damage in the lattice may act as obstacles to dislocation movement. Their effectiveness will depend on both their strength and their number, relative to those obstacles already present in the material. This is evident in the early stages of the in-reactor creep curve for heat treated Zr-2.5 wt % Nb compared with that of cold-worked Zircaloy-2 at 20 000 psi (14.1 kg/mm^2). Irradiation does not appreciably affect the early stages of the creep curve of cold-worked Zircaloy, whose abundant dislocations act as obstacles to slip if the stress is below 30 kpsi (21 kg/mm^2) and whose regions of radiation damage partially recover at 300 °C [17]). However, the in-reactor creep rate of heat treated Zr-2.5 wt % Nb is initially below that of the out-reactor rate and remains so until the out-reactor rate decreases to a lower value [3, 4]). This initially lower in-reactor value is probably caused by the radiation damage, which is stabilized by the niobium, acting as obstacles to dislocation slip. The effect of these obstacles may also depend on the stress since the effectiveness of different types of obstacles can be stress dependent. For example, the creep rate of cold-worked Zircaloy inside a reactor at 300 °C is lower than that outside a reactor for tests at 45 kpsi (31.8 kg/mm^2), but is higher than that outside a reactor for tests at 20 kpsi (14.1 kg/mm^2) [4]).

Apparently, at high stress the radiation-induced obstacles are stronger than other dislocations acting as obstacles to slip. They are also probably the dominant effect that causes the lower creep rate measured in many materials after irradiation. The effect on the creep rate of having two different types of obstacle present is discussed in appendix H. The creep rate is reduced by adding obstacles of another type but the effective activation energy will increase or decrease, depending on whether the activation energy of the second type of obstacle is higher or lower than that of the original obstacles.

6. Discussion

It appears obvious that if radiation growth occurs, the eventual build-up of internal stress will affect the creep rate. It seems equally obvious that the important creep, which relaxes the internal stress within the grains, is occurring during irradiation and is probably due to a tensile stress in the direction of the c-axis. Unfortunately, we do not know this creep rate and will not know it until in-reactor tests on single crystals of this orientation are carried out. However, we do know that it must have a very high stress dependency, with the stress exponent much greater than five, in order to explain the rapid transient effects caused when the reactor is shut-down and to be effective with a reasonable radiation-growth coefficient, as discussed in appendix E. However, it is difficult to explain with this mechanism the rapid increase in creep rate observed when a pre-cept sample is put in the reactor, as in Fidleris's tests R4 and R8 on cold-worked Zircaloy [2]). Because of this, because of the very high value required for n, and because of the high growth rate required to explain the measured creep rates, the enhancement of creep rate caused by a high internal stress due to radiation growth is not considered to be the main mechanism for the high in-reactor creep rate of cold-worked Zircaloy.

Because the internal stress mechanism does not adequately explain the experimental results, other mechanisms are probably responsible. One experiment, which has been done on cold-worked Zircaloy, eliminates two alternate mechanisms [18]). This experiment measured the change in dimensions during the post-irradiation recovery of radiation damage at temperatures up to 380 °C on a piece of pressure tube which had received a creep strain of 0.2% while stressed during irradiation at 270 °C. There should be a creep recovery, i.e. a strain of comparable magnitude to the in-reactor creep strain but in the opposite direction, for each of the following mechanisms for the enhancement of in-reactor creep:

a. Formation of dislocation loops due to aggregated vacancies or interstitials on planes preferentially oriented with respect to the applied stress;
b. Dislocation climb that is limited geometrically without further slip of the dislocation, as in Hesketh's model for graphite [14]).

Experiments, which have just been completed at Chalk River, showed a small positive strain during the recovery of the radiation damage up to 380 °C. Thus, the creep in the reactor could not have been caused by either of these mechanisms. However, it may have been caused by preferred orientation of the large dislocation loops, which are still present at 380 °C. This possibility can probably be examined by direct analysis of the loops using electron microscopy. Preferred loop orientation caused by the crystallographic texture would cause a decrease in circumference during irradiation as the texture showed a predominance of c-axes in the circumferential direction [19]). On recovery, these would produce a positive strain, as observed, but there are probably several other explanations as well. The positive recovery strain was much more evenly spread between 300 °C and 400 °C than was the recovery of the yield stress [17]), which is thought to be due to the recovery of small dislocation loops.

The elimination of most other possible mechanisms for the high creep rate of cold-

worked Zircaloy during irradiation leaves the mechanism of dislocation climb caused by the annihilation of radiation-induced vacancies and interstitials at jogs in dislocations. This mechanism explains the experimentally observed creep rate using reasonable values for the parameters involved, as discussed in appendix F. It also explains both the high activation energy for in-reactor creep measured by Holmes et al. and the transient change in creep rate when a pre-crept sample is put in the reactor or when the reactor is shut down. The effect of pre-irradiation should be negligible except for cases in which the radiation damage regions are acting as the major obstacles to dislocation motion. In this case, which includes cold-worked Zircaloy at high stress and probably also heat treated Zr-2.5 wt % Nb, the diffusion of the point defects to these radiation-induced obstacles may be controlling the creep rate. Using these mechanisms, the creep rate at 300 °C after the reactor has been shut down for several hundred hours may differ from the out-reactor rate due to the internal stress and radiation damage regions that have not yet recovered (which probably includes most of the damage regions in Zr-2.5 wt % Nb but not in Zircaloy). The increase in creep rate when the reactor starts again is due to the mobile point defects and the effect of the added regions of radiation damage whose lifetime is less than several hundred hours at 300 °C. The time required for the creep rate to drop when the reactor is shut down will be determined either by the lifetime of the mobile point defects or by the lifetime of the damage regions which give off point defects during recovery at 300 °C.

The stress and temperature dependence of the in-reactor creep processes that are controlled by mechanisms depending on the migration of radiation-induced point defects is expected to depend on the detailed dislocation arrangement and size distribution of the obstacles. The case of jog-dragging in screw dislocations that is discussed in appendix F is influenced by the stress and temperature dependence of the mobile dislocation density and the relative concentration of sinks for interstitials and vacancies. For general climb of edge dislocations, the creep rate will also depend on the number of places where climb over an obstacle can occur and on the amount of climb required for the dislocation to slip, both of which may depend on the stress and temperature. Some information may be found by comparison with out-reactor creep rates for cases such as Zircaloy in which the creep rate is not controlled by radiation-induced obstacles. However, the continually decreasing rate that is observed out-reactor makes comparison difficult. As suggested in appendix F, the annihilation of a vacancy or an interstitial at a jog in an edge dislocation can easily move the jog past an impurity atom during irradiation but not without irradiation. Thus, comparison with out-reactor creep rates could be very misleading and requires a knowledge of the mechanism of creep outside the reactor, which is not well understood at the present time.

Most mechanisms of in-reactor creep which depend on the arrival of radiation-induced point defects at the dislocations, will produce a lower creep rate if the density of mobile dislocations, relative to the density of other sinks for the defects, is decreased. This reduction can be achieved in two ways: by decreasing the mobile dislocation density, i.e. reducing the amount of prior deformation, or by increasing the number of alternate sinks for the point defects. Adding a solute like niobium, which stabilizes the small regions of radiation damage in zirconium [20]), should reduce the in-reactor creep rate since these damage regions are also sinks for point defects. Fidleris [4]) has reported this effect. Adding molybdenum may stabilize the damage regions to an even higher temperature than does niobium, provided the molybdenum is in solution. From the sequence on the periodic table (zirconium, niobium, molybdenum), one would expect both a larger valence and size effect for additions of molybdenum than for additions of niobium. A search of the literature indicated no evidence that the valence difference is cancelled by a

local electronic state on the molybdenum atoms. It may also be possible to add a solute atom which has an appreciable binding energy to a single vacancy in zirconium. These would then act as a sink for interstitials. The theory does not encourage this approach, however. Calculation of the parameters for the electron screening of a vacancy or solute atom in zirconium indicates a similar radial charge density to that in aluminium [21]). This gives a charge density of zero at the atoms nearest to the vacancy in zirconium. Thus, the binding energy of a vacancy to a solute atom in zirconium is probably low.

With the multitude of possible creep mechanisms that can occur during irradiation of these commercial alloys, it is unlikely that only one mechanism occurs. It is also quite possible for different mechanisms to dominate the process at different stresses and temperatures. At low stresses the effect of a mechanism which is independent of the stress, such as the component of radiation growth in a non-random polycrystal, may be more important than a dislocation slip mechanism which dominates at higher stress due to its stress dependency.

Acknowledgements

I am pleased to acknowledge helpful discussions with V. Fidleris and C. D. Williams of this laboratory and with J. H. Gittus and P. Jones of the Springfield Laboratory, UKAEA. The continued support and encouragement of O. J. C. Runnalls is appreciated.

Appendix A

Radiation damage in zirconium

The average energy transferred from a fission neutron to a zirconium atom, when calculated using the fission spectrum between 0 to 10 MeV and corrected for the changes in anisotropic scattering and cross-section with energy, is 16 keV. Since most fast neutron fluxes are quoted with $E > 1$ MeV, it is interesting to note that 25% of the total energy transferred from the fission neutrons is from neutrons with an energy less than 1 MeV. The average cross-section for elastic scattering of fission neutrons is 4.1 barn. The range of a zirconium atom with 16 keV energy is 85 Å [22]), and it will initially produce about 320 vacancies and interstitials. This gives the fraction of vacant sites within the damage region as 0.12 if the damage region is assumed to be an ellipsoid with length equal to the range and a width of half the length. Since there was no measurable density change caused by a fast neutron irradiation of 6×10^{19} n/cm^2 [23]), most of these defects must have recombined or collapsed to form dislocation loops at room temperature. There were slight anisotropic changes in the lattice parameters of the zirconium produced by the neutron irradiation, however [24]), which indicated that the defects had collapsed into dislocation loops, but the conclusion is uncertain due to the small change measured and the unknown effect of constraint by adjacent grains in the polycrystal. Howe [25]) has bombarded foils of zirconium with 100 keV oxygen ions in the electron microscope. This technique produces radiation damage very similar to that produced by fast neutrons. He obtained results similar to that in aluminium, where large doses are required to observe any change compared with the black spots seen when bombarding copper, cobalt or gold. After long bombardments at room temperature, black spots and dislocation loops are seen. Howe suggests these may be caused by coalescence of defects when the damage regions overlap. In any event, small damage regions are probably present because the yield stress is increased by irradiation. This increase recovers around 300 °C for zirconium and Zircaloy [17]) and around 450 °C for Zr-2.5 wt % Nb [20]).

Electron microscopy of samples irradiated above this recovery temperature or on samples irradiated below and then heated above this temperature, show a larger number of larger dislocation loops and a smaller number of small black spots [26]). Gulden and Bernstein [27]) deduce that the loops resulting from krypton irradiation

are caused by interstitials collecting on prismatic planes. Howe [25]) who has carefully measured several of the larger loops and found both interstitial-type and vacancy-type, concludes that probably both types are present but the uncertainty in the analysis due to the small loop size and surface contamination prevents a definite conclusion.

The migration energies of point defects in zirconium alloys are not well known. The recovery of electrical resistivity after a low temperature deformation [28]) indicates that interstitial zirconium atoms are probably mobile well below room temperature even when oxygen is present. The jump frequency of interstitials at 300 °C is estimated to be

$$\Gamma = \nu \exp(-H_{mi}/kT) = 1 \times 10^{10}/\text{sec},$$

if $\nu = 5 \times 10^{12}$/sec and $H_{mi} = 0.3$ eV. The large amount of recovery also suggests that perhaps vacancies are mobile as well at room temperature. The results of self-diffusion in zirconium have recently been reviewed by Kidson [29]) who indicates that a value of 2.1 eV is a reasonable lower estimate for the activation energy of self-diffusion in α-zirconium. Taking a vacancy formation energy of 1.2 eV, which is estimated from the Debye temperature [30]), the vacancy migration energy is 0.9 eV. This gives vacancies a jump frequency of 5.6×10^4/sec and a lifetime of less than one minute at 300 °C if the sink density is $1.2 \times 10^{16}/\text{cm}^3$. A sink density of about $1 \times 10^{16}/\text{cm}^3$ is expected from Fidleris and Williams' measured loop density in Zircaloy irradiated at 300 °C [2]), taking an average loop diameter of 60 Å and loop density of one fifth their value that was measured at a higher flux level. An additional sink density of $2 \times 10^{15}/\text{cm}^3$ is present from jogs in dislocations on a measured dislocation density of $10^{10}/\text{cm}^2$, assuming a jog spacing of 400 Å. A reasonable upper limit for the vacancy migration energy is obtained by using Ardell's effective melting point of 1858 °K for α-zirconium [24]) and estimating the self-diffusion activation energy as 2.74 eV from this. The above calculation then gives 3 000 h as the average vacancy lifetime in zirconium at 300 °C. The large difference illustrates the need for an accurate measurement of the vacancy migration energy. An average lifetime of 24 h requires a vacancy migration energy of 1.25 eV.

The chemical potential of the excess vacancies and interstitials is equal to $kT \ln (N_p/N_0)$. N_p is the defect concentration. N_0 is the equilibrium defect concentration, which was estimated using a formation energy of 1.2 eV for vacancies and 4.2 eV for interstitials. The defect concentration within the damage region was previously estimated as $N_p = 0.12$ from the number of defects produced per neutron collision and the range of the knocked-on ion. However, some of these vacancies and interstitials will recombine. The common assumption of $N_p = 0.01$, which corresponds to only eight percent of the original defects, seems rather low. However, this conservative value still gives a chemical potential of 0.96 eV for vacancies and 4.0 eV for interstitials within the damage region at 300 °C. The concentration and hence chemical potential of vacancies and interstitials away from the localized damage regions will be lower. During irradiation the concentration of mobile interstitials and vacancies increases until the irradiation time approaches several half lives of the defect concerned. For irradiation times beyond this, the defect formation rate equals the removal rate. The formation rate is $N\sigma_e M\varphi = 5.5 \times 10^{14}/\text{cm}^3 \cdot \text{sec}$ where the number of atoms/cm^3, N, is 4.2×10^{22}; the cross-section, σ_e, is 4.1 barn; the number of displaced atoms per neutron collision, M, is 320; and the fission flux, φ, is 1×10^{13} n/cm$^2 \cdot$sec. The defect removal rate equals $N_p \Gamma_p (C_{sp}/N)$ where N_p is the concentration of the defect considered, Γ_p is its jump frequency and C_{sp} is its sink concentration. Taking $C_{sp} = 1 \times 10^{16}/\text{cm}^3$ for interstitials and vacancies, $\Gamma_{vac} = 5.6 \times 10^4$/sec, and Γ for interstitials $= 1 \times 10^{10}$/sec gives a steady state concentration $N_{vac} = 4 \times 10^{16}/\text{cm}^3$ and $N_{int} = 2.3 \times 10^{11}/\text{cm}^3$ during irradiation at 300 °C. The corresponding chemical potential of these defects is 0.5 eV for vacancies and 2.9 eV for interstitials at 300 °C. If only eight percent of the defects escape from the damage regions,

then the concentrations are reduced to $N_{vac} = 3 \times 10^{15}/cm^3$ and $N_{int} = 1.8 \times 10^{10}/cm^3$. The chemical potentials for vacancies and interstitials away from the damage region at 300 °C are then 0.38 and 2.8 eV, respectively. No correction is necessary for the number of defects that remain to form dislocation loops. These amount to only 10^{-5} of those produced, when estimated from the loops observed after neutron irradiation of Zircaloy at 300 °C [2].

Appendix B

Internal stress in grains of zirconium caused by anisotropy of thermal expansion, irradiation growth, and elastic modulus

In order to conserve continuity of material at the grain boundaries, it is often assumed that all grains deform by the same amount in any particular direction. This amount will, of course, equal the relative change in length of the sample for that direction. Thus the stress in the grain will be proportional to the strain required to force it into this average shape from the shape it would have acquired if it was by itself. These are the internal stresses, which will now be calculated using the usual arguments [31]. The calculated stresses will be the maximum values since local relaxation, which may occur among groups of grains, is not included.

1. Thermal expansion

The difference between the strain of an isolated grain in the direction, i, and the strain of the same grain inside a crystal for a given rise in temperature ΔT, equals $(\overline{\alpha_i} - \alpha_i)\Delta T$ where α_i is the thermal expansion of the isolated grain in the direction i and $\overline{\alpha_i}$ is the average thermal expansion of the polycrystal in the same direction. Pushing this grain back to the average strain, requires a stress

$$\sigma_i = c_i\,(\overline{\alpha_i} - \alpha_i)\,\Delta T,$$

for the one dimensional case, where c_i is the value of Young's modulus in the direction of i. For the three dimensional case

$$\sigma_i = \sum c_{ij}\,(\overline{\alpha_j} - \alpha_j)\,\Delta T, \tag{B1}$$

where j is summed over each of the principal directions when i is one of these directions. For a random polycrystal $\bar{\alpha}$ is independent of the direction, which is the case considered here. Taking $i = 1$ for the close packed a-direction in the basal plane, $i = 2$ for the direction perpendicular to this in the basal plane and $i = 3$ for the direction of the c-axis perpendicular to the basal plane, then $\alpha_1 = \alpha_2$, $c_{31} = c_{32}$ and

$$\left.\begin{aligned} \sigma_1/\Delta T = \sigma_2/\Delta T = c_{11}(\bar{\alpha} - \alpha_1) + c_{12}(\bar{\alpha} - \alpha_2) + \\ + c_{13}(\bar{\alpha} - \alpha_3), \\ \sigma_3/\Delta T = 2c_{31}(\bar{\alpha} - \alpha_1) + c_{33}(\bar{\alpha} - \alpha_3). \end{aligned}\right\} \tag{B2}$$

For a temperature rise of 1 °C in zirconium, this gives a compression of 30.3 psi (2.14 kg/cm^2) in the c-axis direction and a biaxial hydrostatic tension in the basal plane of 20.6 psi (1.45 kg/cm^2). Combining the two together gives an equivalent compressive stress of 51 psi (3.6 kg/cm^2) along the c-axis of the grain with a general hydrostatic tension of 20.6 psi (1.45 kg/cm^2). It is usually assumed that a general hydrostatic stress will not influence deformation by shear. A drop in temperature produces the opposite effects, a tensile stress parallel to the c-axis superimposed on a hydrostatic compression.

2. Irradiation growth

Irradiation growth in a zirconium crystal appears to cause a contraction in the direction of the c-axis at a rate of $\dot{\gamma} = G\alpha\varphi$, where G is the growth constant, α is the fast neutron scattering cross-section and φ is the flux of fast neutrons. There is a corresponding expansion at one half this rate in the direction of the a-axis which keeps the volume constant. However, a grain in the middle of a random unstressed polycrystal should not change its shape. Instead, a stress will build up with increasing irradiation time which introduces an elastic strain opposite in direction and equal in magnitude to the growth strain. The elastic stress can be calculated in exactly the same

way as that caused by the temperature change. In fact, one interesting and possibly useful feature is that the stress introduced by a temperature drop is in exactly the same crystallographic direction as that produced by irradiation growth. The equation for growth corresponding to eq. (B1) is

$$\sigma_i = \sum_j c_{ij} (\overline{G_j} - G_j)\, (\alpha\varphi)\, \Delta t, \qquad \text{(B3)}$$

where Δt is the time of irradiation. For a random polycrystal $\overline{G_j}$ is independent of the direction i, and for growth $G_1 = G_2 = -\frac{1}{2}G_3$ making $\overline{G} = 0$ for a random polycrystal. Therefore, the equations for the stress due to growth corresponding to eqs. (B2), are

$$\left.\begin{aligned} \sigma_1 = \sigma_2 &= (\alpha\varphi)\, \Delta t[-c_{11} G_1 - c_{12} G_2 - c_{13} G_3] \\ &= (\alpha\varphi)\, \Delta t\, G_3\, [\tfrac{1}{2}(c_{11} + c_{12}) - c_{13}], \\ \sigma_3 &= (\alpha\varphi)\, \Delta t[-2c_{31} G_1 - c_{33} G_3] \\ &= (\alpha\varphi)\, \Delta t\, G_3[c_{31} - c_{33}]. \end{aligned}\right\} \qquad \text{(B4)}$$

Taking $\alpha = 4$ barn, $\varphi = 10^{13}$ fast n/cm^2·sec, $G_3 = -1$/neutron, $\Delta t = 1$ h, and using Fisher's values for elastic constants of zirconium at 300 °C gives [32])

$$\sigma_1 = \sigma_2 = -0.81 \text{ psi/h } (57 \text{ g/cm}^2\text{·h}),$$

$$\sigma_3 = 1.88 \text{ psi/h } (132 \text{ g/cm}^2\text{·h}).$$

Therefore, combining the two together gives an equivalent tensile stress increase along the c-axis direction of 2.7 psi/h (190 g/cm^2·h) with a superimposed hydrostatic compression of 0.81 psi/h (57 g/cm^2·h). Using these figures, one can calculate the irradiation time required to increase the internal stress to a limiting value at which the creep rate of the grains for a tensile stress parallel to the c-axis equals the growth rate in the c-axis direction. Unfortunately, no creep tests on oriented single crystals of Zircaloy have yet been done. If the creep rate in this direction decreases with time, as it does for a polycrystal, then the limiting value of the stress will increase accordingly. The time required to reach a tensile stress of 20 000 psi at a flux of $\varphi = 10^{13}$ fast n/cm^2·sec assuming no relaxation by creep is 7400 h which corresponds to an integrated flux of 2.7×10^{20} fast n/cm^2.

3. Anisotropic elastic modulus

The stress within a grain will be calculated in terms of the externally applied stresses, $\overline{\sigma_a}$, $\overline{\sigma_b}$ and $\overline{\sigma_c}$, which are parallel to the three principal axes x_a, x_b and x_c respectively. The subscripts a, b, c are used for principal axes to avoid confusion with the numbers 1, 2, 3 which are being used for the crystallographic axes of a grain. It will be assumed that E_j, the strain in the direction j for each grain, will equal that for the whole sample $\overline{E_j}$. Therefore, for each grain

$$\sigma_i = \sum_j c_{ij} E_j, \qquad \text{(B5)}$$

but

$$\overline{E_j} \equiv \overline{E_j} = \sum_k \overline{s_{jk}}\, \overline{\sigma_k}, \qquad \text{(B6)}$$

where the $\overline{s_{jk}}$ is the average value of the elastic compliance for the whole sample.

For the case of a uniaxial external load, $\overline{\sigma_a}$, applied in the direction x_a, putting eq. (B6) into eq. (B5) gives

$$\sigma_i = \sum_j c_{ij}\, \overline{s_{ja}}\, \overline{\sigma_a}, \qquad \text{(B7)}$$

or written in full:

$$\left.\begin{aligned} \sigma_a/\overline{\sigma_a} &= c_{aa}\, \overline{s_{aa}} + c_{ab}\, \overline{s_{ba}} + c_{ac}\, \overline{s_{ca}}, \\ \sigma_b/\overline{\sigma_a} &= c_{ba}\, \overline{s_{aa}} + c_{bb}\, \overline{s_{ba}} + c_{bc}\, \overline{s_{ca}}, \\ \sigma_c/\overline{\sigma_a} &= c_{ca}\, \overline{s_{aa}} + c_{cb}\, \overline{s_{ba}} + c_{cc}\, \overline{s_{ca}}. \end{aligned}\right\} \qquad \text{(B7)}$$

Since the terms with a bar above them apply to average values over the whole sample, they will depend on the direction of the applied stress with respect to the crystallographic texture axes. For a polycrystal with random texture $\overline{s_{aa}} = E^{-1}$ and $\overline{s_{ba}} = \overline{s_{ca}} = -\nu/E$, where $E = 1.18 \times 10^7$ psi (8.3×10^5 g/cm^2) and $\nu = 0.352$ are the Voigt averages calculated from Fisher's measured elastic constants for zirconium at 300 °C [32]). Using these values, the internal stress will be calculated in grains of three different orientations, those with their c-axes at angles of 0°, 52° and 90° to the direction of the applied stress. The first two of these

correspond to the directions with maximum and minimum values for Young's modulus and hence will have the extreme values of internal stress.

Case 1: Grains with their c-axis, x_3, parallel to the direction of applied stress, x_a. The stress is calculated from eq. (B7) replacing a by 3, b by 1, and c by 2, in all terms without the bar above them. For a random polycrystal, this gives $\sigma_a = 1.34\ \overline{\sigma_a}$, $\sigma_b = -0.100\ \overline{\sigma_a}$, $\sigma_c = -0.100\ \overline{\sigma_a}$.

For plastic deformation by a shear process, these stresses are equivalent to a tensile stress of $1.44\ \overline{\sigma_a}$ in the direction of the applied stress (which, of course, is in the direction of the c-axis of this particular grain) and a superimposed hydrostatic compression equal to $0.10\ \overline{\sigma_a}$.

Case 2: Grains with c-axis 52° from the direction of the applied stress. The elastic moduli, c_{ij}, that are required for use in eq. (B7), were calculated for this orientation using Hearmon's equations [33]). Putting these and the Voigt values for the average random polycrystal into eq. (B7) gives $\sigma_a = 0.908\ \overline{\sigma_a}$; $\sigma_b = 0.067\ \overline{\sigma_a}$; and $\sigma_c = 0.032\ \overline{\sigma_a}$. For a shear process this is equivalent to a uniaxial tensile stress of magnitude $0.903\ \overline{\sigma_a}$ in a direction within one degree of x_a, superimposed on a hydrostatic tension of $0.05\ \overline{\sigma_a}$. Resolved on the crystallographic directions of this grain, the stresses are $0.50\ \overline{\sigma_a}$ in a direction parallel to the c-axis of the grain, i.e. perpendicular to the basal plane, and $0.76\ \overline{\sigma_a}$ maximum with $0.032\ \overline{\sigma_a}$ minimum for directions lying in the basal plane.

Case 3: Grains with their a-axis, x_1, parallel to the direction of the applied stress, x_a. The stress is calculated from eq. (B7) replacing a by 1, b by 2, and c by 3, in all terms without the bar above them. This gives $\sigma_a = 0.96\ \overline{\sigma_a}$; $\sigma_b = 0.11\ \overline{\sigma_a}$; and $\sigma_c = -0.16\ \overline{\sigma_a}$ which corresponds to a uniaxial tensile stress equal to $\overline{\sigma_a}$ but oriented about 10° from the x_a axis, superimposed on a hydrostatic compression of $0.03\ \overline{\sigma_a}$.

Thus the range of stresses effective in a shear process including all grain orientations is from $0.9\ \overline{\sigma_a}$ to $1.44\ \overline{\sigma_a}$ with an average value of $\overline{\sigma_a}$.

4. Application and interdependence of these internal stresses

The principal reason for calculating these internal stresses was to apply the results to the creep of reactor components in which the internal stress due to radiation growth is present in addition to the applied stress. This application is discussed in appendix E. However, other interesting applications to zirconium alloys also arise and these are discussed below.

4.1. *Deformation of zirconium by cooling to −196 °C*

The local stress on cooling from 400 °C to −196 °C is a tensile stress of 30 kpsi (21.2 kg/mm^2) along the c-axis of the grains. If this is sufficient to cause twinning, it may be a very useful technique to reduce the maximum internal stress caused by irradiation growth. Reed-Hill et al. [34]) have shown that $\{11\bar{2}1\}$ twins produced by tensile deformation of pure zirconium at −196 °C can accommodate strain at room temperature by increasing the width of the twins, i.e. by stress-induced twin boundary migration. If this same migration occurs at a lower stress than plastic creep in irradiated Zircaloy at 300 °C, then the internal stress introduced by irradiation growth will saturate at a lower value, thus reducing its contribution to the in-reactor creep rate. Of course, the general creep rate both inside and outside the reactor may also be increased by introducing these twins.

4.2. *The yield drop in a tensile test after strain ageing*

Weinstein found a yield drop for tests of polycrystalline zirconium at high temperature but none at low temperature [35]). The loss of the yield drop at lower temperature may be due to the internal stresses introduced during cooling from the strain-ageing temperature. These stresses may move some of the dis-

locations away from the solute atoms that pin them and it may also cause yielding in many of the grains before the normal yield stress is reached, thus reducing the sharp yield point. Tests on single crystals would not have these internal stresses. Thus, one would expect a larger yield drop at lower temperature for a single crystal oriented for slip.

4.3. *The effect of a prior stress in a different direction*

The stress due to elastic anisotropy was calculated for the case in which an external load was applied to a polycrystal that was initially stress free. The same internal stress distribution, but in the opposite direction, will occur when a sample is unloaded after plastic deformation has raised the stress in all the grains to a uniform value. Thus, prior deformation by tube drawing will introduce local stresses in grains which, if not removed by annealing, will affect experiments that are sensitive to these stresses. This is one possible reason for the different primary creep in tubes under pressure and tension. Of course, other internal stresses such as those causing the normal Bauschinger effect inside the grains may also be important.

4.4. *Creep steps*

The introduction of creep steps, i.e. short periods of rapid strain during a creep test, may be due to the build-up of stress in some grains when the others are deforming by creep. If these undeformed grains tend to deform at a critical stress by twinning or a yield drop effect, then a period of rapid creep may be initiated.

4.5. *Comparison of samples with different heat treatments*

In general, when a sample is annealed for an appreciable time at a high temperature, the internal stress is reduced to a low value by creep. However, if the sample is cooled at a rate that inhibits the creep relaxation of the stress introduced by the temperature drop, a tensile stress along the c-axis with a magnitude of 51 psi/°C (3.6 kg/cm^2·°C) will develop in each grain. Great care must therefore be taken when comparing samples of different final annealing temperature and cooling rate in experiments such as irradiation growth and primary creep which are affected by internal stress.

4.6. *Superimposing other internal stresses to investigate those of one type*

The principle of superposition of elastic stresses suggests several interesting experiments to investigate any one method for introducing stress. For instance, if irradiation growth is controlling the in-reactor creep rate, then the time to attain the steady creep rate, i.e. to saturate the internal stress due to growth, will be reduced if the prior annealing temperature is above the irradiation temperature. Also, if the temperature is changed after reaching the steady creep rate in the reactor, the local stress caused by radiation growth will be increased by a temperature drop and decreased by a temperature rise.

In all these calculations the effects of localized complex stresses near the grain boundaries have been ignored. If these cover an appreciable volume of the grain, the above arguments are still correct but other stresses probably of a lower magnitude will also exist.

Appendix C

Energy terms involved in the formation of dislocation loops during irradiation

There are four significant energy terms that may be important for the formation of prismatic dislocation loops by the condensation of radiation-induced vacancies and interstitials. The first is the energy available, which is the chemical potential of the vacancies or interstitials caused by their supersaturation. The values during irradiation of zirconium alloys with a fission flux of 1×10^{13} n/cm^2·sec at 300 °C are about 0.96 eV per vacancy and 4.0 eV per interstitial, as given in appendix A. The

other three terms are the elastic strain energy, the stacking fault energy, and the work done against a stress during the formation of the dislocation loop. Because the stacking fault energy is not well known, the other terms will be calculated and the energy available for the stacking fault will be their difference.

The elastic strain energy of a prismatic loop depends on the elastic moduli, which are anisotropic in hexagonal metals. In the absence of a general solution [36]), the loop energy will be estimated from that of the two types of dislocations in a square-shaped loop. The values of K for dislocations that are required to form prismatic loops on the prism and basal planes and shear loops on the prism plane, were calculated from Foreman's [37]) eq. (27) and are given in table C1. The K values for the shear

TABLE C1

Anisotropic energy factor K, for straight dislocations.

Plane of dislocation loop	Dislocation		K (10^{11} dyne/cm^2)			
	Line direction	b direction	Be	Zr	Mg	Zn
Basal plane vacancy loop	$10\bar{1}0$	0001	16.6	5.19	2.5	3.37
Prism plane vacancy loop	$\bar{1}2\bar{1}0$	$10\bar{1}0$	15.4	4.73	2.47	5.47
	0001	$10\bar{1}0$	14.5	4.13	2.40	7.81
Prism plane shear loop	0001	$\bar{1}2\bar{1}0$	14.5	5.32	2.42	7.78
	$\bar{1}2\bar{1}0$	$\bar{1}2\bar{1}0$	14.7	3.36	1.67	4.97

TABLE C2

Energy terms in the formation of dislocation loops by vacancy condensation.

Metal	Dislocation loop			K (10^{11} dyne/cm^2)	E_{dis}, eq. (C1) (10^{-11} erg)	E_{vac}, eq. (C2) (10^{-11} erg)	$\left[\frac{E_{vac}-E_{dis}}{\pi r^2}\right]$ (erg/cm^2)
	Plane	b	$\|b\|$ (10^{-8} cm)				
Be	0001	$(c/2)$ (0001)	1.78	16.6	12.7	41.5	2300
	$10\bar{1}0$	$(a/2)$ $(10\bar{1}0)$	1.97	15.1	13.5	46.0	2600
	$10\bar{1}0$	$(a/6)$ $(\bar{1}210)$	1.14	14.6	5.4	–	–
	$11\bar{2}0$	$(a/3)$ $(11\bar{2}0)$	2.28	15.1	17.03	53.1	2880
Zr	0001	$(c/2)$ (0001)	2.56	5.19	7.0	21.1	1130
	$10\bar{1}0$	$(a/2)$ $(10\bar{1}0)$	2.79	4.43	6.8	23.0	1290
	$10\bar{1}0$	$(a/6)$ $(\bar{1}2\bar{1}0)$	1.61	4.34	2.75	–	–
	$11\bar{2}0$	$(a/3)$ $(11\bar{2}0)$	3.22	4.43	8.4	26.7	1460
Mg	0001	$(c/2)$ (0001)	2.60	2.5	3.44	35.8	2590
	$10\bar{1}0$	$(a/2)$ $(10\bar{1}0)$	2.77	2.43	3.93	38.4	2760
	$10\bar{1}0$	$(a/6)$ $(\bar{1}2\bar{1}0)$	1.60	2.02	1.30	–	–
	$11\bar{2}0$	$(a/3)$ $(11\bar{2}0)$	3.20	2.43	4.55	44.3	3180
Zn	0001	$(c/2)$ (0001)	2.46	3.37	4.27	30.8	2120
	$10\bar{1}0$	$(a/2)$ $(10\bar{1}0)$	2.30	6.64	7.59	28.8	1700
	$10\bar{1}0$	$(a/6)$ $(\bar{1}2\bar{1}0)$	1.33	6.37	3.04	–	–
	$11\bar{2}0$	$(a/3)$ $(11\bar{2}0)$	2.66	6.64	9.5	33.4	1910

loop on the prism plane are those calculated in the same way by Tyson [38]). Elastic isotropy, which exists in the basal plane, produces equal K values for any direction in the plane and hence equal K values for prismatic loops on any prism plane.

Table C2 gives the values for the strain energy of dislocation loops using the equation

$$E_{dis} = 0.5\ rKb^2 \ln(r/r_0), \qquad (C1)$$

where b is the magnitude of the Burgers' vector, r is the loop radius, which is taken to be 20 Å, and r_0 is assumed equal to b to include an estimate of the core energy.

The energy available from the vacancies that condense to form the loop of 20 Å radius is

$$E_{vac} = Ns\mu_{vac}\pi r^2, \qquad (C2)$$

where N is the number of atoms per unit volume, s is the interplanar spacing, and $\mu_{vac} = 0.96$ eV $= 1.53 \times 10^{-12}$ erg is the chemical potential for vacancies in a damage region. Values for E_{vac} are also given in table C2. It is seen that the energy available from the vacancies easily supplies that required for the dislocation strain energy. The effect of a stress of 20 kpsi (14.1 kg/mm^2) applied parallel to b would only contribute an energy to the loop formation of 0.5×10^{-11} erg, which is small compared with the other terms. The final column in table C2 gives the value for the energy per unit area that is available for the stacking fault within the loop. The high values indicate that loops can probably form on many different planes. Once formed, however, their stability depends on the chemical potential of vacancies during irradiation, which for zirconium at 300 °C is about 40% of the value assumed within the spike region (appendix A). Even this lower value allows an appreciable stacking fault energy. However, if the stacking fault energy is dominant, the calculated values for E_{dis} that are given in table C2 indicate that perfect loops would form directly by vacancy condensation on $\{11\bar{2}0\}$ planes in preference to vacancy condensation plus a shear on $\{10\bar{1}0\}$ planes.

Appendix D

The nut-and-bolt analogy for internal stress *

1. Tensile case

The increase of internal stress caused by radiation growth is illustrated by the stress in the bolt and tube of fig. 1 when the nut is tightened. Tightening the nut introduces an internal stress I, which is tensile in the bolt and compressive in the tube. Continued tightening increases the stress until yielding occurs. If yielding occurs in one member before the other, then the stress in each will equal the flow stress of the yielding member, and strain produced by further tightening of the nut will be accommodated by plastic deformation of the yielding member. This case is shown graphically by the solid lines in fig. 2a, where I_0 is the value of the internal stress. If the nut is tightened at a rate causing a uniform strain rate $\dot{\varepsilon}$, then the rate of increase in stress is $\dot{I} = E\dot{\varepsilon}$, where E is the elastic modulus. The time to reach the yield stress σ_y is $(\sigma_y/\dot{I})$. Of course, if the yield stress depends on the

* I am indebted to J. H. Gittus who told me of this analogy and attributed it to A. H. Cottrell.

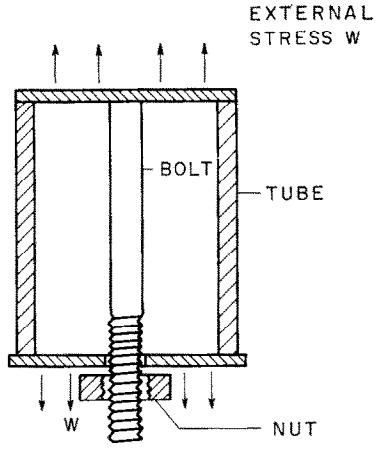

Fig. 1. The nut-and-bolt analogy for internal stress using a concentric bolt and tube. Tightening the nut puts a tensile stress in the bolt and a compressive stress in the tube. These are of equal magnitude if the bolt and tube have the same cross-section and elastic modulus. An external tensile stress, w, may be applied to the whole assembly.

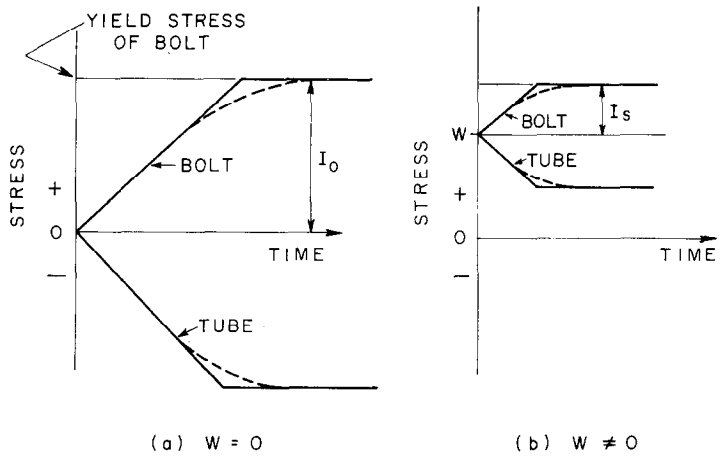

Fig. 2. The solid line shows the total stress in the bolt and tube as the nut is tightened at a constant rate. I is the value of the internal stress in the bolt. The dotted line shows the corresponding case if plastic creep occurs while the nut is slowly tightened.

rate of straining, the applicable value is that at the imposed strain rate, $\dot{\varepsilon}$. This corresponds to the case of an internal stress built up by radiation growth when there is no applied stress.

If a tensile stress w is applied to both the rod and tube before the nut is tightened, as shown in fig. 1, then tightening the nut will cause yielding at a lower value of internal stress and after a shorter time than the previous case. This is shown by the solid lines in fig. 2b, where I_s is the internal stress. The limiting value of I_s is obviously affected by the applied stress. This corresponds to the case of internal stress introduced by irradiation growth when there is an applied stress.

In the previous cases normal tensile strain rates have been assumed where the effect of creep can be ignored. If the internal stress is increased very slowly it can be reduced by a plastic creep strain. This will produce a change of internal stress with time that corresponds to the dotted curves of fig. 2. Since we are only considering the yield stress that corresponds to that of the imposed strain rate, the final or saturation value of internal stress will be that required to produce plastic creep at a rate equal to the strain rate imposed by the tightening nut. If this is in the region of steady state creep, then the final value is constant. If it is in the region where the creep rate normally decreases continually with time (which corresponds to work hardening at normal strain rates), then the internal stress will continue to rise at the rate required to accommodate the imposed strain by creep. Of course, the creep in both the tube and the bolt need to be considered. The creep accommodating the tightening nut is the elongation in the bolt minus the elongation in the tube, which is proportional to the maximum creep rate minus the average.

Appendix E

The effect of an internal stress distribution on the creep rate

Internal stresses of a magnitude estimated in appendix B are introduced in polycrystalline zirconium alloys by a temperature change, load change or irradiation. Their effect on the creep rate will be estimated by assuming the internal stresses in the grains lies between the values $-I$ and $+I$ with a distribution that yields a uniform distribution of creep rates for the individual grains. Thus the total stress in the grains, w_t, which is the sum of the applied stress, w, plus the internal stress will vary from $w_t = (w - I)$ to $w_t = (w + I)$. This simple stress distribution was chosen in order to keep the

physical arguments clear without too much mathematical clutter, and to reasonably estimate the magnitudes involved. A more realistic distribution has been used by Blackburn [7]), who assumed the creep rate in each grain depended on the deviator stress component. The purpose of the present calculation is to check one of his major assumptions (that the limiting value of the internal stress is independent of the applied stress) and to estimate the change in creep rate with strain when the internal stress is not maintained. In sect. 1, the creep rate is calculated assuming each grain creeps according to the relation

$$\dot{\varepsilon}_t = A\,(w_t)^n, \qquad \text{(E1)}$$

under the influence of a steady internal stress. This is applicable to the in-reactor case after an irradiation time sufficient to raise the internal stress to its steady value. In many cases, however, the internal stress is not steady. It usually is introduced by a change in temperature or load and is relaxed during creep because grains of higher stress creep faster than the average. This is also the case for pre-irradiated samples or for in-reactor samples when the reactor is shut down. The change in creep rate with strain for this case is calculated in section 2. The effect of an applied stress on the limiting internal stress produced by radiation growth, and hence on the limiting in-reactor creep rate due to these internal stresses, is discussed in section 3. In most of the calculations, the creep rate when an internal stress is present is estimated in terms of an enhancement factor, f, which is the ratio of creep rates with and without the internal stress, when the same applied stress is present.

1. Effective creep rate when a distribution of stresses exists

If the effective creep rate is taken as the average creep rate of all the grains, then using eq. (E1), one gets

$$\dot{\varepsilon}_{\text{eff}} = \frac{\int a_t \dot{\varepsilon}_t \,\mathrm{d}\dot{\varepsilon}_t}{\int a_t \,\mathrm{d}\dot{\varepsilon}_t} = \frac{\int a_t \dot{\varepsilon}_t (\delta\dot{\varepsilon}_t/\delta w_t)\,\mathrm{d}w_t}{\int a_t (\delta\dot{\varepsilon}_t/\delta w_t)\,\mathrm{d}w_t},$$

where a_t is the frequency distribution, which is assumed constant for $0<(w-I)<w_t<(w+I)$ and zero outside this range. Using these as the limits of integration, gives

$$\dot{\varepsilon}_{\text{eff}} = \tfrac{1}{2} A\, w^n \left\{ \frac{[1+(I/w)]^{2n} - [1-(I/w]^{2n}}{[1+(I/w)]^n - [1-(I/w]^n} \right\}. \qquad \text{(E2)}$$

Therefore, the creep enhancement factor, f, is

$$f \equiv \frac{\dot{\varepsilon}_{\text{eff}}}{\dot{\varepsilon}} = \tfrac{1}{2} \left\{ \frac{[1+(I/w)]^{2n} - [1-(I/w)]^{2n}}{[1+(I/w)]^n - [1-(I/w]^n} \right\}, \qquad \text{(E3)}$$

where $\dot{\varepsilon}$ is the creep rate if all grains just have the applied stress, w. Values of f for various values of n and I/w are given in table E1, using this equation.

The usual conclusion of no creep rate enhancement when $n=1$ is evident. It is also evident that both n and I/w must be appreciable in order to have a large enhancement in the creep rate. The last column gives the corresponding values of f when $n=5$ using Blackburn's eq. (10) as calculated by Hesketh [11]). The simple unidirectional stress distribution assumed here gives values about 40% higher than those calculated using Blackburn's plasticity theory for the three-dimensional stress distribution. The exact difference probably depends on the values of n and I/w.

In some cases, as when the applied stress is changed during the test, there is not a symmetrical distribution for the number of grains

Table E1

Values for the creep enhancement factor, f, calculated from eq. (E3).

I/w	f					f, for $n=5$ from fig. 3, ref. [11])
	$n=1$	$n=2$	$n=3$	$n=4$	$n=5$	
0.1	1.0			1.06	1.10	
0.2	1.0			1.24	1.41	1.22
0.4	1.0	1.15		1.98	2.72	1.98
0.8	1.0			5.25	9.45	6.05
1.0	1.0	2.0	4.0	8.0	16.0	11.0

as a function of stress. The effect of a skewed distribution can be estimated from a simple example which crudely represents the stress distribution from 7.6 to 11.7 kpsi that is produced by elastic anisotropy when the tensile stress is reduced from the initial value of 18 kpsi (12.7 kg/mm^2) to the final value of 11 kpsi (7.7 kg/mm^2). Let one sixth of the grains have a stress $w_t = w\ (1-0.2)$ and five sixths have a stress $w\ (1+0.04)$. Assume, as previously, that the effective creep rate is the average creep rate of the grains using eq. (E2) with $n=4$. The effective creep rate will have a creep enhancement factor of $f=1.04$ for the assumed distribution which is skewed to the low stress side. A similar distribution skewed to the high stress side has a creep enhancement factor of 1.05. Thus, there may be a creep enhancement even when the stress distribution is skewed to low stresses.

2. Change in the creep enhancement with strain

In many cases the internal stress is not maintained during creep. Those grains having the highest total stress, $w_t=(w+I)$, will creep at the rate $\dot{\varepsilon}_{max}=A\ (w+I)^n$, which is higher than the average rate given by eq. (E2). Thus the internal stress in these grains will be reduced at a rate that depends on the difference of their creep rate and the average, times the elastic modulus: i.e.,

$$\dot{I} = -E[\dot{\varepsilon}_{max} - \dot{\varepsilon}_{eff}]. \qquad \text{(E4)}$$

The problem is to find the value of the creep enhancement factor, f, with strain, ε_{eff}. One simple method is to calculate the new value of internal stress I from eq. (E4), after a time interval required to give an increment of strain. Taking the increment of strain as k times the

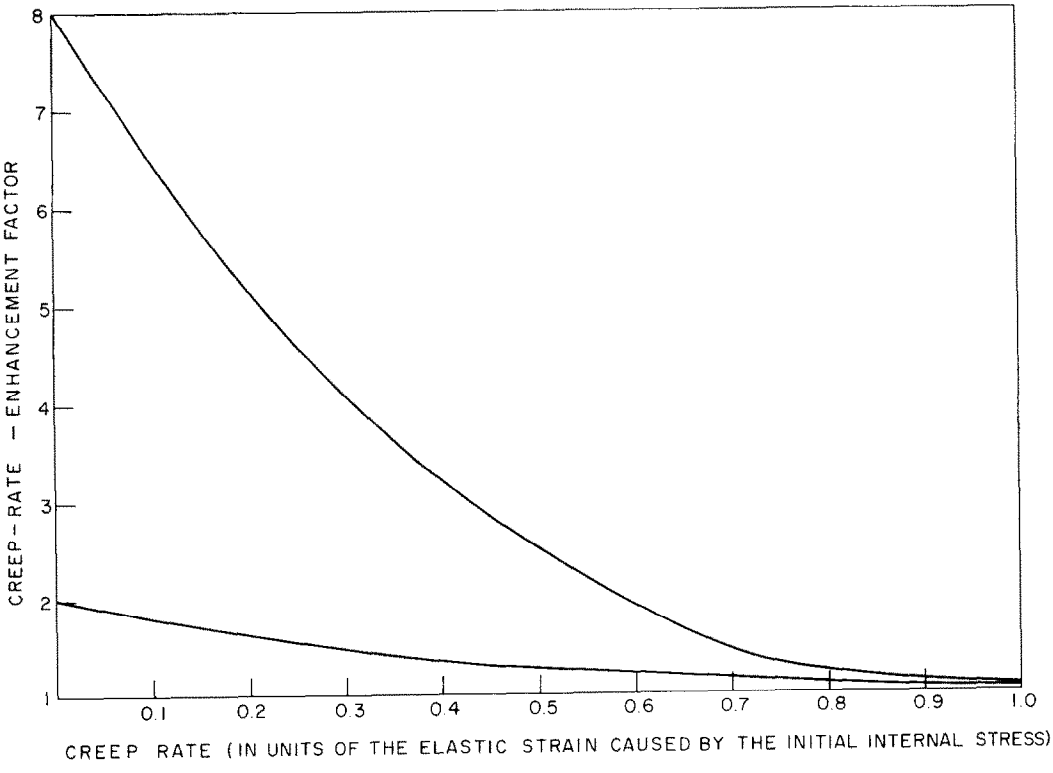

Fig. 3. Decrease in the creep-rate-enhancement factor, f, with increasing strain assuming $I=w$ at $\varepsilon=0$. Curves are given for two values of n, the stress exponent of the creep rate. For the lower curve $n=2$ and for the upper curve $n=4$.

elastic strain produced by the initial internal stress I_0 gives

$$\Delta\varepsilon_{\text{eff}} = kI_0/E = \dot{\varepsilon}_{\text{eff}}\Delta t. \qquad \text{(E5)}$$

Hence

$$\Delta I = \dot{I}\Delta t = (\dot{I}kI_0)/(E\dot{\varepsilon}_{\text{eff}}). \qquad \text{(E5)}$$

Putting $\dot{\varepsilon}_{\text{eff}} = f\dot{\varepsilon} = Aw^n$ into eqs. (E4) and (E5) and solving for ΔI gives

$$\Delta I = kI_0\{1 - f^{-1}[1 + I/w]^n\}.$$

Hence, if I_a = internal stress after the a^{th} time interval, then

$$I_a = I_{a-1} + kI_0\{1 - f_{a-1}^{-1}[1 + I_{a-1}/w]^n\}, \qquad \text{(E6)}$$

which can be put into eq. (E3) to give the corresponding creep enhancement factor.

An example was calculated in which the initial internal stress equalled the applied stress. Fig. 3 shows the expected decrease of f with strain during the creep of this sample. The values used were $I_0 = w = 20$ kpsi (14.1 kg/mm^2) and $n = 4$ or $n = 2$.

The effect of a prior irradiation on the creep can be estimated from fig. 3 as this internal stress is ninety percent of that expected from a pre-irradiation of 3×10^{20} fast n/cm^2 in the unstressed state (from appendix B). The calculations indicate an average enhancement of 5 (for $n = 4$) or 1.6 (for $n = 2$) during a plastic creep strain of half the elastic strain. The elastic strain for a load of 20 kpsi (14.1 kg/mm^2) is 0.17%. Thus, when the total strain (elastic plus plastic) of a sample without prior irradiation is 0.26%, the sample with prior irradiation

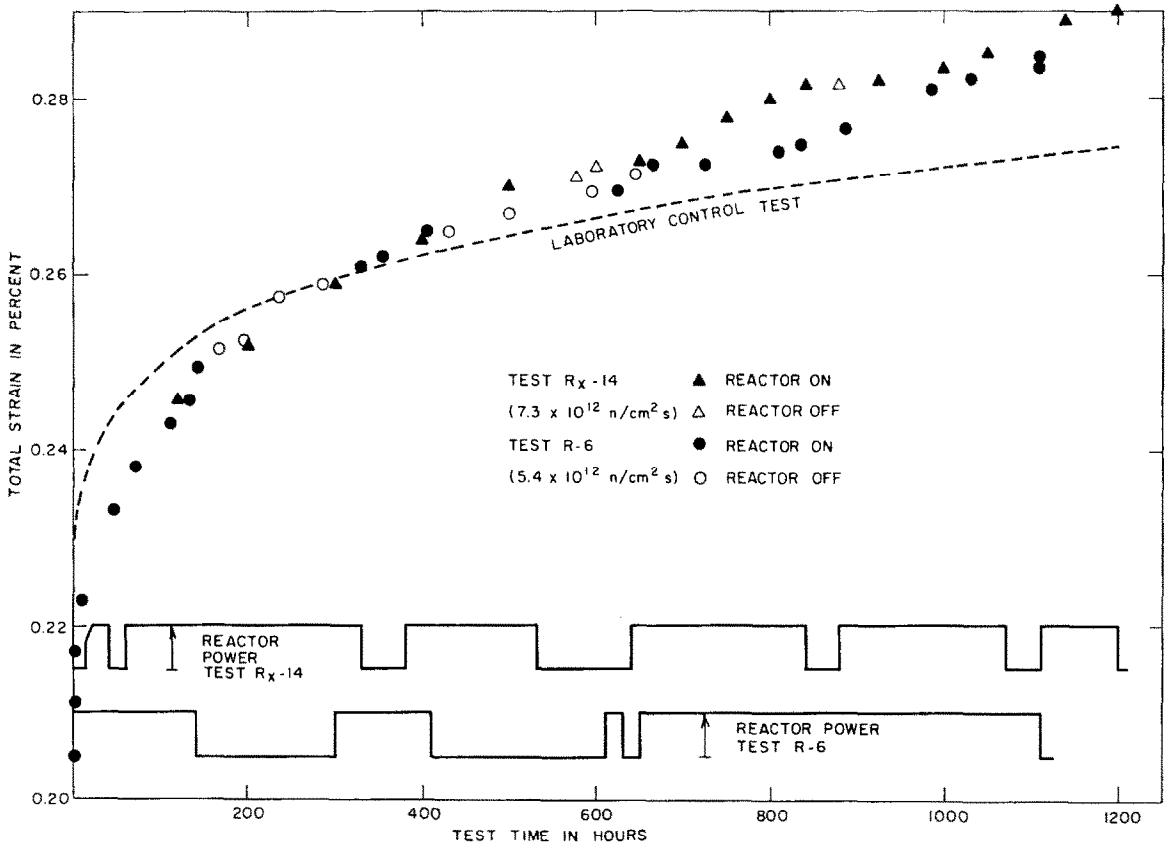

Fig. 4. In-reactor creep curves of cold-worked Zircaloy. Sample Rx-14 was pre-irradiated with 3×10^{20} fast n/cm^2 at 300 °C. Sample R-6 was not pre-irradiated. Both tests were at 300 °C using a stress of 20 kpsi (14.1 kg/mm^2).

should have strained 0.62% if $n=4$ or 0.31% if $n=2$. Fig. 4 shows the creep curves for samples in Fidleris's test Rx-14, that was pre-irradiated to 3×10^{20} fast n/cm^2, and R-6 that was not pre-irradiated. Both are the same within experimental error, which indicates that either the internal stress does not build up at the calculated rate during irradiation, or that the assumptions made in this type of calculation are invalid. Both samples will have other smaller internal stresses, which are estimated in appendix B. These will alter the absolute values somewhat but should not give the zero effect of pre-irradiation that was found experimentally.

The same magnitude and direction of internal stress is obtained by dropping the temperature by 400 °C. Thus the effect of this initial internal stress on the creep rate at 300 °C could be investigated by comparing samples rapidly cooled with those very slowly cooled from 700 °C. The very slow cooling must be at a rate in which the internal stresses are recovered by creep. Perhaps a more realistic experiment is to compare the creep rate of zirconium samples cooled rapidly from a number of different temperatures. Of course, effects of solute or precipitates must be excluded.

The above sample is also applicable to the decrease in creep rate when the reactor is shut-down. If the enhanced creep rate is caused by an internal stress of this magnitude, then the rate of enhancement will decrease with plastic creep strain when the reactor is shut off, in the manner shown in fig. 3. Fidleris's test R-6 on cold-worked Zircaloy showed a reduction in creep rate by a factor of seven within approximately 100 h after the reactor was shut-down [2]). This time corresponds to a creep strain less than 3×10^{-5} which is less than two percent of the elastic strain introduced by an internal stress of 20 kpsi (14.1 kg/mm^2). Table E1 indicates that a stress of this order is necessary in order to explain a creep rate enhancement by a factor of seven. Thus, the large enhancement of the creep rate and its rapid drop when the reactor is turned off do not appear to be adequately explained by a model using internal stresses unless the value of n is significantly greater than 4.

3. The effect of an applied stress on the limiting internal stress produced by radiation growth

In Blackburn's second case, which is the one used by Hesketh [11]), it is assumed that the increase in internal stress due to radiation growth is independent of the applied stress. His asymptotic value for the internal stress is that required to give a creep rate equal to the growth rate. A more reasonable assumption is to include the applied stress in this calculation and assume the internal stress increases with radiation time until the difference between the creep rate of the grains oriented for maximum total stress and the creep rate of the sample is equal to the growth rate, i.e. the asymptotic value or saturation value of the internal stress, I_s, is reached when

$$\dot{\varepsilon}_{max}-\dot{\varepsilon}_{eff}=\dot{\gamma}, \qquad \text{(E7)}$$

where $\dot{\varepsilon}_{max}=A(w+I_s)^n$, $\dot{\varepsilon}_{eff}$ is the effective creep rate of the sample when the stress distribution is present, and $\dot{\gamma}$ is the radiation growth rate considered in appendix B. Using the simple stress distribution from $(w-I)$ to $(w+I)$, the value of $\dot{\varepsilon}_{eff}$ is given in eq. (E2). Putting this and the above relation for $\dot{\varepsilon}_{max}$ into eq. (E7) gives

$$(1+I_s/w)^n-(1-I_s/w)^n=2\dot{\gamma}/\dot{\varepsilon}, \qquad \text{(E8)}$$

where $\dot{\varepsilon}\equiv Aw^n$. Eq. (E8) can be solved explicitly for I in terms of w if n is an integer. When the applied stress is zero, then $A(I_s)^n=\dot{\gamma}$. Defining this value for the saturation internal stress as $I_{s0}=(\dot{\gamma}/A)^{1/n}$, then the values of I_s from eq. (E8) can be put in terms of this for comparison. The solutions, for integral n, are:

$$\left.\begin{aligned}
&n=1 \quad I_s=I_{s0},\\
&n=2 \quad I_s=(I_{s0})^2/(2w),\\
&n=3 \quad I_s=I_{s0}(2)^{-\frac{1}{3}}\{[1+y^{\frac{1}{2}}]^{\frac{1}{3}}+[1-y^{\frac{1}{2}}]^{\frac{1}{3}}\},\\
&\qquad\qquad \text{where } y=1+4(w/I_{s0})^6,\\
&n=4 \quad I_s=I_{s0}^{\frac{1}{4}}w^{-\frac{1}{4}}(2)^{-1}\{[1+z^{\frac{1}{2}}]^{\frac{1}{4}}+\\
&\qquad\qquad +[1-z^{\frac{1}{2}}]^{\frac{1}{4}}\},\\
&\qquad \text{where } z=1+(64/27)\,(w/I_{s0})^8.
\end{aligned}\right\} \qquad \text{(E9)}$$

Values of I_s/I_{s0} for the case $w=I_{s0}$ are given in table E2 with the resulting creep rate enhancement factor calculated from eq. (E3). Obviously, the saturation value for the creep enhancement factor can be grossly over-estimated if the effect of the applied stress is not included when calculating the saturation value for the internal stress. The corresponding time to reach this value will also be overestimated.

TABLE E2

Values of I_s/I_{s0} calculated from eq. (E9) with $w=I_{s0}$ and the corresponding values of f_s and f_{s0}, the saturation creep rate enhancement including and excluding the effect of the applied stress, from eq. (E3).

n	I_s/I_{s0}	f_s	f_{s0}
1	1	1.0	1.0
2	0.5	1.25	2.0
3	0.33	1.32	4.0
4	0.24	1.35	8.0

APPENDIX F

The velocity of jogs in dislocations during irradiation

A recent publication by Gibbs and Turnbull[39]) has clarified the arguments for the formation of vacancies at jogs in dislocations. They combine the two processes of vacancy formation at the jog on the atomic scale, with diffusion of these vacancies away from the jog on a macroscopic scale. In the present case, the effect of irradiation and the different geometry of an edge jog in a screw dislocation will be considered. A simple case will be considered first in order to keep the physical arguments clear.

Consider the curve for the enthalpy H_v of a vacancy (including vibrational entropy terms) with position in the lattice, fig. 5. Position number one acts as a vacancy source or sink. By definition, the probability of a vacancy being present in this position is unity. Position number two is a normal lattice position. H_{mv} is the energy required to move a vacancy from one lattice site to another and H_{fv} is the energy normally required to form a vacancy. The jump frequency of vacancies from position one to Z neighbouring sites corresponding to position two, is Z times the product of the probability of finding a vacancy in position one (unity), and the probability of having it jump to position two,

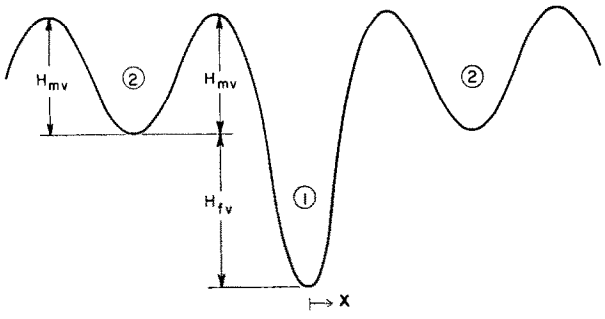

Fig. 5. Change in enthalpy of a vacancy with distance x away from the vacancy source. Position 1 is the vacancy source. Position 2 represents a normal lattice site adjacent to the source. H_{fv} and H_{mv} are the energies required to form and move the vacancy.

$$\nu \exp\left[-(H_{fv}+H_{mv})/(kT)\right],$$

where ν is the atomic vibration frequency, k is Boltzmann's constant and T is in °K. If there is work τlb^2 done by an applied shear stress τ as the vacancy is formed, then this is subtracted from the H_{fv} term. An applied shear stress will cause the dislocation to curve ahead of the jog, which puts a force τlb in the direction of jog motion [40]), where l is the distance between jogs and b is the interatomic distance. Thus, a jog that moves in the direction of the applied stress by producing vacancies, will produce them at a rate

$$\begin{aligned} dN_v/dt &= Z\nu \exp\left[-(H_f+H_m-\tau lb^2)/(kT)\right] \\ &= Zmb^{-2}D_{sv} \exp\left[(\tau lb^2)/(kT)\right], \end{aligned}$$

where $D_{sv} \equiv b^2\nu m^{-1} \exp\left[-(H_f+H_m)/(kT)\right]$ is the coefficient for self-diffusion via a vacancy mechanism. Similarly, a jog that moves in the opposite direction to the applied stress by producing vacancies has

$$dN_v/dt = Zmb^{-2}D_{sv} \exp\left[-(\tau lb^2)/(kT)\right].$$

In a similar way, the vacancy flow from the Z positions of type two into position one,

equals Z times the probability of finding a vacancy in position two (N_v/N) times the probability of the vacancy jumping into position one ($\nu \exp[-(H_{mv})/(kT)]$), where N is the total number of type-two lattice sites per unit volume and N_v is the number of vacancies per unit volume in these sites. But

$$N_v/N = (N_v/N_{v0})(N_{v0}/N),$$

where

$$N_{v0}/N \equiv \exp[-(H_{fv})/(kT)].$$

Thus, the net number of vacancies produced at a jog that moves forward by vacancy production is

$$dN_v/dt = \qquad \text{(F1)}$$
$$= Zmb^{-2}D_{sv}\{\exp[(\tau lb^2)/(kT)] - N_v/N_{v0}\}.$$

Similarly, the net number of vacancies produced at a jog that moves backward by vacancy production is

$$dN_v/dt = \qquad \text{(F2)}$$
$$= Zmb^{-2}D_{sv}\{\exp[-(\tau lb^2)/(kT)] - N_v/N_{v0}\}.$$

These are the same equations given by Gibbs and Turnbull [39]) and also by Friedel [41]) when N_v/N_{v0} is replaced by its equivalent $\exp[\mu_v/(kT)]$, where μ_v is the chemical potential for vacancies. The jogs can also move by interstitial formation or absorption, and equations analogous to eqs. (F1) and (F2) are obtained with the v for vacancy replaced by i for interstitial. The interstitial terms are negligible for the out-reactor case but become significant during irradiation.

The value of N_v/N_{v0} for sites adjacent to the jog is now found by setting the net vacancy flow given by eq. (F1) equal to the net flow from these adjacent sites into the surrounding region, as suggested by Gibbs and Turnbull [39]). Rosenthal's solution [42]) for diffusion from a point source moving with velocity w in the x direction is

$$N_p = N_p^{\infty} + q(4\pi D_p R)^{-1} \exp[-(wx)/(2D_p)] \cdot \exp[-(wR)/(2D_p)],$$

where N_p is the defect concentration at position with coordinates x and R in the moving coordinate system, N_p^{∞} is the defect concentration at $R = \infty$, $q = dN_p/dt$ equals the number of defects produced per second at the source,

$$D_p = b^2\nu_m^{-1} \exp[-H_{mp}/(kT)],$$

is the diffusion coefficient of the defect concerned. As we want the average value of N_p at all sites adjacent to the source, i.e. $R = b$, we need to average the first exponential term for all values of x on the circle $R = b$. Because there are symmetrical points at positive and negative values of x, the average value of the exponential term will be $\cosh[(\alpha wb)/(2D_p)]$ where α lies between zero and unity, probably near one third. Using this average value and $R = b$ in the above equation gives

$$N_p = N_p^{\infty} + (dN_p/dt)(4\pi D_p b)^{-1} \cosh[(wb)/(6D_p)] \cdot \exp[(-wb)/(2D_p)]. \qquad \text{(F3)}$$

In practice, p will be replaced by v for the case of vacancies and by i for the case of interstitials.

Equating dN_v/dt for vacancy flow in eq. (F3) with that in eq. (F1) and solving for N_v gives

$$N_v = \frac{N_{v0}AZm D_{sv} \exp[(\tau lb^2)/(kT)] + N_v^{\infty}N_{v0}b^2}{N_{v0}b^2 + AZm D_{sv}},$$

where

$$A = (4\pi D_v b)^{-1} \cosh[(wb)/(6D_v)] \cdot \exp[-(wb)/(2D_v)].$$

Putting this value of N_v back into eq. (F3) for vacancies, gives

$$dN_v/dt = \frac{Zm\, D_{sv}b^2\{\exp[(\tau lb^2)/(kT)] - (N_v^{\infty}/N_{0v})\}}{1 + ZmQ(4\pi b^3)^{-1} \cosh[(wb)/(6D_v)] \exp[-(wb)/(2D_v)]}, \qquad \text{(F4)}$$

where Ω = volume per atom = $0.7\,b^3$ for zirconium and metals with a fcc structure. Thus the coefficient in front of the cosh term is about $(12)\cdot(6)\cdot(0.7)\cdot(4\pi)^{-1}=4$.

The jog velocity $w=b(\mathrm{d}N_\mathrm{v}/\mathrm{d}t)$. Putting this into the left side of eq. (F4) results in an equation for the jog velocity which cannot be solved explicitly. However, two limiting cases arise. When $wb \ll D_\mathrm{v}$ the cosh and exponential terms equal unity, which makes the dominator equal to five. When $wb \gg D_\mathrm{v}$ the product of the cosh and exponential terms gets very small, which makes the denominator equal to unity. Thus

$$\mathrm{d}N_\mathrm{v}/\mathrm{d}t = y_\mathrm{v} Z m D_\mathrm{sv} b^{-2}\{\exp\,[(\tau l b^2)/(kT)] - - (N_\mathrm{v}^\infty/N_\mathrm{v0})\}, \qquad \text{(F5)}$$

with y_v ranging between the limiting values 0.2 when $wb \ll D_\mathrm{v}$ and 1.0 when $wb \gg D_\mathrm{v}$.

A comparison of eq. (F5) with eq. (F1) under normal out-reactor creep conditions, $N_\mathrm{v}^\infty = N_\mathrm{v0}$, shows the magnitude of the error in assuming that the rate of diffusion of the excess vacancies away from the region near the jog is unimportant, i.e. assuming that $N_\mathrm{v}=N_\mathrm{v0}$ in eq. (F1). The two equations are identical when the jog velocity is sufficient to leave the region of non-equilibrium vacancy concentration, i.e. $wb \gg D_\mathrm{v}$. However, for a jog moving at a slower velocity, the use of eq. (F1) with $N_\mathrm{v}=N_\mathrm{v0}$ will give a value of $\mathrm{d}N_\mathrm{v}/\mathrm{d}t$ and hence of creep rate, that is too large by a factor up to five. Barrett and Nix [43] in their calculation of jog velocity obtain eq. (F5) with $y_\mathrm{v}=0.25$.

Consider now the supersaturated case normally occurring during irradiation. The velocity of a jog that moves forward by creating vacancies or absorbing interstitials has a resultant velocity

$$W_1 = b\left(\frac{\mathrm{d}N_\mathrm{v}}{\mathrm{d}t}\right) - b\left(\frac{\mathrm{d}N_\mathrm{i}}{\mathrm{d}t}\right).$$

The equation for the rate of interstitial absorption is the negative of eq. (F5), with all the subscripts v for vacancy replaced by i for interstitial, and a negative sign in front of τ since the stress inhibits interstitial formation. Thus W_1 becomes

$$W_1 = Zmb^{-1}\{y_\mathrm{v}D_\mathrm{sv}\exp\,[(\tau l b^2)/(kT)] - - y_\mathrm{v}D_\mathrm{sv}N_\mathrm{v}^\infty/N_\mathrm{v0} + y_\mathrm{i}D_\mathrm{si}N_\mathrm{i}^\infty/N_\mathrm{i0} - y_\mathrm{i}D_\mathrm{si}\cdot\exp[-(\tau l b^2)/(kT)]\}. \qquad \text{(F6)}$$

The magnitude of these terms can be estimated from the following parameters: $Z=12$, $m=6$, $b=3.2\times10^{-8}$ cm, $y_\mathrm{v}=0.2$. $D_\mathrm{sv}=(5\times10^{12})\times\times(3.2\times10^{-8})^2(6)^{-1}\exp\,[-2.1/k(573)]=3\times10^{-22}$ cm$^2\cdot$sec, $\tau=6.9\times10^8$ dyn/cm^2 for tensile stress 20 000 psi, $l=2\times10^{-6}$ cm, i.e. $\tau l b^2=0.88$ eV, $N_\mathrm{v0}=(4.3\times10^{22})\exp\,[-1.2/(k573)]=1.3\times10^{12}/$ cm^3, $y_\mathrm{i}-0.2$, $D_\mathrm{si}-(5\times10^{12})(3.2\times10^{-8})^2(6)^{-1}\cdot\cdot\exp[-4.5/(k573)]=1.7\times10^{-43}$ cm^2/sec, $N_\mathrm{i0}=(4.3\times10^{22})\exp\,[-4.2/(k573)]=4.2\times10^{-15}$/cm^3. The value of N_v^∞, which is the steady state concentration of vacancies, is estimated in appendix A to be $3\times10^{18}\varphi/C_\mathrm{sv}$, where φ is the fission neutron flux in n/cm$^2\cdot$sec and C_sv is the sink concentration for vacancies. Similarly, $N_\mathrm{i}^\infty=1.8\times10^{13}\ \varphi/C_\mathrm{si}$ for interstitials. When these parameters are put into eq. (F6), the jog velocity equals $Zmb^{-1}=2\times10^9$ times the contribution from each of the four terms, which are:

$$y_\mathrm{v}D_\mathrm{sv}\exp\,[(\tau l b^2)/(kT)]=3.2\times10^{-15}$$

due to vacancy production at the jog, minus

$$y_\mathrm{v}D_\mathrm{sv}N_\mathrm{v}^\infty/N_\mathrm{v0}=-1.4\times10^{-16}\ \varphi/C_\mathrm{sv}$$

due to vacancy absorption at the jog, plus

$$y_\mathrm{i}D_\mathrm{si}N_\mathrm{i}^\infty/N_\mathrm{i0}=1.4\times10^{-16}\ \varphi/C_\mathrm{si}$$

due to interstitial absorption at the jog, minus

$$y_\mathrm{i}D_\mathrm{si}\exp\,[-(\tau l b^2)/(kT)]=-7\times10^{-52}$$

due to interstitial production at the jog. The resulting velocity, deduced from the first term is $W_1=6\times10^{-6}$ cm/sec.

There are two very important features in this result. If $\varphi=10^{13}$ n/cm$^2\cdot$sec and $C_\mathrm{sv}=10^{16}$/cm^3 as discussed in appendix A, then the neutron flux has a negligible effect on this jog, whose velocity is still determined by vacancy production at the jog. However, at lower temperatures where N_v^∞ is higher, or at lower stress or smaller activation volume where $\tau l b^2$ is lower,

the radiation may affect the velocity of this jog. The second important feature is that even at low temperature or stress, the effect of irradiation will depend on the difference between the density of sinks for interstitials and vacancies.

The equation for the velocity, W_2, of jogs that normally move forward by vacancy absorption or interstitial production is identical to eq. (F6) with i's replaced by v's, and vice versa. Using the same values for the parameters, the resulting velocity is $Zmb^{-1} = 2 \times 10^9$ times the contribution from each of the following four terms:

$$y_i D_{si} \exp[(\tau l b^2)/(kT)] = 3 \times 10^{-36}$$

due to interstitial production at the jog, minus

$$y_i D_{si} N_i^{\infty}/N_{i0} = -1.4 \times 10^{-16} \varphi/C_{si}$$

due to interstitial absorption at the jog, plus

$$y_v D_{sv} N_v^{\infty}/N_{v0} = 1.4 \times 10^{-16}) \varphi/C_{sv}$$

due to vacancy absorption at the jog, minus

$$y_v D_{sv} \exp[-(\tau l b^2)/(kT)] = -1.8 \times 10^{-28}$$

due to vacancy production at the jog. It is apparent that the main two terms contributing to the velocity of this type of jog, which normally moves by absorbing vacancies, are the absorption of radiation-induced vacancies and interstitials. The resulting velocity is much lower than that of the previous type of jog and depends on the difference between the concentration of sinks for vacancies and interstitials. However, it is probably appreciably higher than that for the out-reactor case in which $N_v^{\infty}/N_{v0} \equiv 1$. In fact, the sink concentrations only have to differ by 0.04% in a nominal sink concentration of $10^{16}/cm^3$, for the jog velocity during irradiation to triple that of jogs in unirradiated samples. Such small differences are certainly beyond the scope of calculated sink concentrations.

Once the velocity of the jogs is known, it is necessary to estimate the velocity of the dislocations that contain these jogs in order to find the creep rate. The above calculations indicate that even for the in-reactor case, the velocity of jogs that move forward by vacancy absorption is less than 0.1% the velocity of those that move forward by vacancy emission. When both types of jog are present on each dislocation, one would expect the slower moving jog to be most important in determining the dislocation velocity. Barrett and Nix [43]) used the average jog velocity in their initial paper. A recent letter has clarified their case [44]). Holmes [45]) calculated the local defect concentration necessary to impose the same velocity on both jogs, but assumed that the concentration was the same at both types of jog. Some of these calculations assume the applied stress produces an equal force on all jogs, which is not correct. The force is caused by the line tension of the curved dislocation at the jog [40]). Even if both types of jogs did initially have the same force, the faster jog would move ahead, thus reducing the forward force caused by the dislocation curvature at that type of jog. This will reduce its velocity until it matches that of the slower jog. During this process the slower jog will speed up by an amount depending on the local jog distribution. If there are equal numbers of both types of jog, the maximum effect is to double the effective dislocation length between the slower moving jogs. The situation is analogous to that when two different types of obstacles hold up the dislocations, as discussed in appendix H.

The above argument suggests that the slower moving jogs, which are those moving forward by vacancy absorption, dominate the creep rate if it is controlled by this mechanism. Because such a small difference in interstitial and vacancy sink concentrations will enhance the velocity of these jogs, the relatively low in-reactor creep rates indicate that nearly all the interstitials are annihilated at radiation-induced vacancies, or that another mechanism is limiting the creep rate. If this jog mobility is still the rate-limiting process, even during irradiation, then the stress and temperature dependence of the creep rate must arise through their effects on the mobile dislocation density and the

relative sink concentrations. Unfortunately, both of these are difficult to even estimate with any certainty for an impure material in which dislocations and point defects may be held at many different impurities. Comparison of the equation given for this jog velocity during irradiation and the in-reactor creep rate of 5×10^{-7}/h measured by Fidleris's test Rx-14 on cold-worked Zircaloy [4]), which used a fission neutron flux of 1×10^{13} n/cm^2·sec gives $C_{sv}^{-1} = = C_{si}^{-1} + \dot{\varepsilon}(\varrho Z m q 1.4 \times 10^{-16})^{-1}$ when the creep rate $\dot{\varepsilon} = \varrho b v$, where ϱ is the mobile dislocation density and v is the dislocation velocity, which was assumed equal to that of the slower moving jog. Putting in $C_{si} = 10^{16}$/cm^3 as estimated in appendix A, gives a value of $C_{sv} = 0.999\ C_{si}$ if $\varrho = 10^{10}$/cm^3, which is the total dislocation density measured by electron microscopy [2]). If the mobile dislocation density is reduced to something like 10^6/cm^2 by strain ageing, then this measured in-reactor creep rate requires $C_{sv} = 0.07\ C_{si}$ if jog dragging limits the creep rate.

The only case considered so far has been the movement of the jogs in screw dislocations, i.e. the climb of edge dislocations which are of only one or two atomic lengths. The stress assisting or inhibiting the movement was the shear stress causing curvature in the screw dislocation. Similar arguments also occur when considering the climb rate of a longer edge dislocation, in that the climb is produced by the movement of a jog of one atomic length along the dislocation. A tensile stress σ_{xx} parallel to the Burgers' vector of the dislocation produces a force on the jog that aids the movement of those jogs moving by vacancy creation at the jog, i.e. moving in a direction that enlarges the area of the half plane of atoms forming the edge dislocation. Thus, this σ_{xx} will replace τ in all the equations considered and l will equal b. The major difference in this case is that only one type of jog can occur. Thus eq. (F6), with these modifications, represents the velocity of jogs moving in a direction to create vacancies or absorb interstitials. In this case, $\sigma_{xx} \approx \tau$ for dislocations on planes at 45° to the applied tensile axis. The values of y_v and y_i will be of the same magnitude as those considered previously but the absolute value will probably be slightly different due to the different diffusion geometry caused by the attraction of vacancies to the whole length of the edge dislocation [39]). Taking $\tau = \sigma_{xx}$, $l = b$, gives $\tau l b^2 = 0.014$ eV and $\exp(\tau l b^2/kT) = 1.32$. Using the previous values for the other parameters causes the first term in the bracket of eq. (F6) to become $y_v D_{sv} \exp(\tau l b^2/kT) = 8 \times 10^{-23}$. This will be one of the major terms in the case of creep outside the reactor, if it is controlled by a climb process, but is probably much smaller than the next two terms for the in-reactor case. Once again, the jog velocity appears to be dominated by the radiation-induced vacancies and interstitials. In fact, for the in-reactor jog velocity to equal the out-reactor velocity [both found from eq. (F6)], requires a difference in sink concentration for vacancies and interstitials of only one part in 10^5. This sensitivity to the effect of irradiation on the difference between the sink concentration is similar to that previously calculated for the velocity of slower moving jogs in screw dislocations. All the additional arguments given in that case also apply in this one.

The in-reactor creep rate caused by the movement of jogs in edge dislocations compared to that in screws has one additional feature. A similar creep effect is expected whether the edge dislocations climb away from their obstacles by enlarging or reducing the area of their half plane. Thus, the in-reactor creep rate will depend on the magnitude of the jog velocity and not on its sign. Thus, it depends only on the magnitude of the difference in sink concentration, whereas a higher in-reactor creep rate determined by the velocity of jogs in screw dislocations required the interstitial sink concentration to be higher than that for vacancies.

One interesting feature of this velocity of jogs in edge dislocations is the small energy term of 0.014 eV, which is contributed by the applied stress per atomic jump of the jog. This jog could probably be held up by an impurity atom in the case of creep outside the reactor.

However, inside the reactor the energy contributed by the absorption of a vacancy or interstitial at the jog could probably free it from the impurity atom. Thus the attraction of the jog to impurity atoms, which would cause the creep rate to continually decrease with time outside the reactor, would have little effect during irradiation.

Appendix G

The effect of solute atoms on creep in zirconium

1. Atmosphere drag

If the solute atoms are attached to the dislocation, its velocity will be reduced to the diffusion velocity of the solute. Since the dislocation exerts a force F on the solute atom, the net jump frequency of the solute in the direction of F will give a velocity of

$$v = 2Db^{-1} \sinh [(Fb)/(2kT)], \qquad (G1)$$

which reduces to $DF/(kT)$ when $Fb \ll 2kT$ [46]). D is the normal solute diffusion coefficient and b its jump distance. But $F = \tau b^2/n$, where $n = C_0 \exp [E_b/(kT)]$ is the fraction of atomic sites along the dislocation that are filled with solute if C_0 is the atomic fraction of dissolved solute and E_b is the binding energy of the solute atom to the dislocation. However, the dislocation will break away from the solute if $Fb > E_b$. Thus, the resulting creep rate is $\dot{\gamma} = \varrho bv$ where ϱ is the density of mobile dislocations. Combining these equations gives a tensile creep rate

$$\dot{\varepsilon}_{drag} = \qquad (G2)$$
$$= \varrho D \sinh [(\sigma b^3)/(4C_0 kT)] \exp [E_b/(kT)],$$

which is valid up to a tensile stress

$$\sigma_{max} = (2E_b C_0/b^3) \exp [E_b/(kT)], \qquad (G3)$$

where $\dot{\varepsilon} = \frac{1}{2}\dot{\gamma}$ and $\sigma = 2\tau$. Taking $E_b = 0.2$ eV, $\varrho = 10^{10}/\text{cm}^2$, $\sigma = 20$ kpsi $= 14.1$ kg/mm^2 and the tabulated value of D at 300 °C gives the values of $\dot{\varepsilon}_{drag}$ and σ_{max} for the various solutes in Zircaloy given in table G1. Unfortunately, the binding energy of solutes to dislocations in zirconium is not known. Therefore, the calculated values are those expected if the binding energy is around 0.2 eV. Even with this reasonably high binding energy, dislocations will break away from atoms of iron, chromium and nitrogen at reasonable stresses unless they form a precipitate on the dislocation.

2. Pinning of moving dislocations by solute atoms

A moving dislocation is held up briefly at various obstacles in the lattice. If the time at the obstacles is greater than the time required for solute to diffuse to the dislocation, then the dislocation will be pinned in position by the solute atoms. Friedel [47]) gives a pinning time of

$$t_{pin} = kTb^2 [DE_b(3C_0)^{3/2}]^{-1}.$$

Table G1

Zirconium creep rate for atmosphere drag, $\dot{\varepsilon}_{drag}$, eq. (G2), maximum stress for atmosphere drag σ_{max}, eq. (G3) and maximum creep rate for solutes to pin moving dislocations $\dot{\varepsilon}_{pin}$, eq. (G4).

Solute	Concentration C_0	$D_{300\,°C}$ (cm^2/sec)	$\dot{\varepsilon}_{drag}$/h ($\sigma = 14.1$ kg/mm^2)	σ_{max} (kg/mm^2)	$\dot{\varepsilon}_{pin}$ (h^{-1})
hydrogen	0.007	1.6×10^{-6}	2×10^{8}	16	1×10^{4}
oxygen	0.007	3.4×10^{-19}	4×10^{-5}	16	2×10^{-9}
nitrogen	0.000 26	3.4×10^{-19}*		0.6	
tin	0.01 [48])	1×10^{-19}*	6×10^{-6}	23	1×10^{-9}
niobium	0.01	1×10^{-19}*	6×10^{-6}	23	1×10^{-9}
iron	0.000 65 [48])	1×10^{-19}*		1.5	
chromium	0.000 35 [48])	1×10^{-19}*		0.8	

* Assumed value.

The normal resting time of dislocations at obstacles depends on the dislocation configuration. In cold-worked Zircaloy the dislocations are fairly evenly distributed. Thus, the dislocation velocity $v = d/t$ can be estimated using $d = \varrho^{-\frac{1}{2}}$ where d is the distance the dislocations move between obstacles, and t is the time spent at the obstacles. The resulting creep rate is

$$\dot{\gamma} = \varrho_m b v = \varrho_m b t^{-1} \varrho^{-\frac{1}{2}},$$

where ϱ_m is the mobile dislocation density. Replacing t by the pinning time gives the critical creep rate

$$\dot{\varepsilon}_{pin} = \varrho_m D E_b (3C_0)^{3/2} [2kTb\varrho^{\frac{1}{2}}]^{-1}. \quad \text{(G4)}$$

If $\dot{\varepsilon} > \dot{\varepsilon}_{pin}$ then a dislocation torn free of its atmosphere will remain free until it meets an exceptionally strong obstacle. Taking $\varrho = 10^{10}/cm^2$, $\varrho_m = 10^6/cm^2$, $E_b = 0.2$ eV gives the values for $\dot{\varepsilon}_{pin}$ shown in table G1.

The uncertainty in the value for the binding energy and for the diffusion coefficient for tin and niobium make the calculated results very uncertain. Nevertheless, it is clear that oxygen, tin, and niobium may affect the creep rate by forming atmospheres around dislocations. Their low values for $\dot{\varepsilon}_{pin}$ indicate that a dislocation free of its atmosphere will not be repinned until it is held up at one of the stronger obstacles. This may be the reason for the large strain introduced in a creep test by a temperature cycle, as the cycle will produce internal stress that may free the dislocation from its atmosphere. The estimates also show that dissolved hydrogen should have a negligible effect on creep or even normal tensile tests, since the hydrogen can move readily with the dislocations at 300 °C. However, if hydride precipitates on the dislocation the calculations do not apply.

Appendix H

1. Obstacles to dislocation motion

A large effort is presently being spent trying to understand and predict the effect of obstacles that impede the slip of dislocations. The arguments are reasonably clear when only one type of obstacle is present [49]). The creep rate is equal to

$$\dot{\varepsilon} = nPAb, \quad \text{(H1)}$$

where n is the number of slip sources per unit volume; i.e. the number of places where a slip dislocation is held up, P is the frequency that a slip source operates, A is the area slipped by a dislocation before being held up again, and b is the Burgers' vector of the dislocation. P equals the frequency ν that the source is in a position to slip times the probability of it having sufficient thermal energy, H. Thus, using Boltzmann statistics

$$\dot{\varepsilon} = nAb\nu \exp(-H/kT) = nAb(\bar{t})^{-1}, \quad \text{(H2)}$$

where $\bar{t}$, the average time that the slip source requires to operate, is

$$\bar{t} = P^{-1} = \nu^{-1} \exp(H/kT). \quad \text{(H3)}$$

The activation energy may depend on the applied stress. Mott used the local curvature of the dislocation to estimate the force that it exerts on an obstacle [40]). This force, τlb, times d, the distance it moves through the obstacle under thermal activation, is equal to the work done by the applied stress; where τ is the effective shear stress on the slip plane and l is the distance between obstacles on the slip plane. The product lbd is called the activation volume, v. Thus the thermal activation energy is

$$H = H_0 - v\tau. \quad \text{(H4)}$$

The value of H_0, d and hence v will decrease with increasing stress if the barrier is not abrupt [50]). Also a random barrier distribution will cause l and hence v to decrease with increasing stress [51]). Thus a knowledge of these parameters allows one to estimate the creep rate. Conversely, the measured creep properties give values of these parameters which give an indication of the creep mechanism.

The situation is more complex when more than one type of obstacle holds up the dislocation. Assuming all the dislocations are

similarly affected, the creep rate can still be determined from eq. (H2) if $\bar{t}$ is summed over the various types of obstacles. Considering two types of obstacle gives

$$\left.\begin{aligned}\bar{t} = [N_1 \nu_1^{-1} \exp[H_1/(kT)] + \\ + N_2 \nu_2^{-1} \exp(H_2/kT)](N_1+N_2)^{-1},\end{aligned}\right\} \quad \text{(H5)}$$

where N_1 and N_2 are the numbers of obstacles of type 1 and 2 per unit area of slip plane.

Putting this value of $\bar{t}$ into eq. (H2) gives

$$\left.\begin{aligned}\dot{\varepsilon} = nAb\nu_1 \exp[-H_1/(kT)] \cdot \\ \cdot \{N_1(N_1+N_2)^{-1} + \\ N_2(N_1+N_2)^{-1} \nu_2 \nu_1^{-1} \exp[(H_2 - \\ - H_1)/(kT)]\}^{-1}.\end{aligned}\right\} \quad \text{(H6)}$$

Thus, the effective activation energy found by comparing eqs. (H6) and (H2) is

$$H_{eff} = H_1 + [H_2 - H_1]\{1 + \\ + N_1\nu_2(N_2\nu_1)^{-1} \exp[(H_1-H_2)/(kT)]\}^{-1}. \quad \text{(H7)}$$

The second factor in eq. (H6) is a measure of the reduction in creep rate when the second type of obstacle is added. Similarly, the second term in eq. (H7) gives the change in effective activation energy caused by introducing the second type of obstacle. It is apparent from these equations that even though the creep rate is reduced when the second type of obstacle is added, the effective activation energy may be either larger or smaller than H_1 depending on the sign of $(H_2 - H_1)$.

These equations have ignored the change in n, A, H_1 and H_2 caused by introducing the second type of obstacle. The product nA is equal to $(\varrho/l_e)l_e^2 = \varrho l_e$, where ϱ is the density of mobile dislocations and l_e is the effective length of dislocation between the barriers. The value of l that determines the activation energies from eq. (H7) may also be decreased by introducing the second type of obstacle. There are two limiting cases that can be used for this correction. If both types of obstacle have similar strength, then the effective value of l in all terms will be determined by the total number of obstacles on the slip plane (as was used by Koppenaal and Kuhlmann-Wilsdorf [52]) to explain the increase in yield stress when both radiation damage regions and dislocations act as obstacles). This gives

$$l_c = (l_1^2 + l_2^2)^{\frac{1}{2}}, \quad \text{(H8)}$$

where l_1 is the distance between obstacles of type 1 on the slip plane. However, if their strengths are not similar, then the dislocation has time to bow out between those particles with large $\bar{t}$. Thus, the effective length of dislocation cutting the stronger obstacles is determined from the separation of the strong obstacles alone, but the effective length for the weaker obstacles is obtained from eq. (H8). These modified values of l could then be put into the various terms of eqs. (H6) and (H7). An equation for the effective activation volume can be found by replacing H_1 and H_2 in eq. (H7) using their expanded form of eq. (H4) and differentiating with respect to stress.

2. Measurement of activation energy and volume

There are two basic methods to measure activation energies. The first is by the change in the rate of the process when the temperature is changed. This "slope-change" method works well if the defect configuration is the same at both temperatures; a condition which is not satisfied by Zircaloy during irradiation near 300 °C. The mechanical strength of irradiated Zircaloy recovers in a few hours at temperatures above 300 °C [17]. Thus, the small defect clusters or platelets that cause the increase in mechanical strength due to irradiation must be unstable at these temperatures. In this case, the concentration of both these defect clusters and the mobile point defects will depend on the temperature of irradiation. Increasing the temperature will supersaturate these defects. Thus, any creep mechanism which is enhanced by the annihilation of the excess defects will have a large change in creep rate for a small temperature rise, which from eq. (H2) would indicate a large activation energy. The high

value measured during the in-reactor creep of cold-worked Zircaloy [15]) indicates that the creep rate is enhanced either by the removal of these defect clusters as obstacles or by the excess point defects produced when the clusters break up. Because of this complication, however, an absolute value for the effective activation energy and activation volume is better obtained from the steady creep rates obtained during irradiation. Using the usual equation to represent the in-pile creep rate

$$\dot{\varepsilon} = A\tau^r \exp\{-[H_0 - v(\tau - \tau_G)]/(kT)\},$$

τ^r represents the stress dependence of the mobile dislocation density and the distance between obstacles. τ_G is the long range stress field. The parameters can be found from the following curves:

(a) The curve ln $\dot{\varepsilon}$ versus τ has a slope $r\tau^{-1} + v/(kT)$. Thus, the values of r and v can be found by comparing the slopes of the curves from measurements taken at two different temperatures.

(b) The curve ln $\dot{\varepsilon}$ versus $(kT)^{-1}$ has a negative slope equal to $H = [H_0 - v(\tau - \tau_G)]$. Thus, the values of $(H_0 + v\tau_G)$ can be found knowing v from part (a) and this activation energy H. The dependence of $(H_0 + v\tau_G)$ on the applied stress, τ, can be found by measuring the temperature dependence of the creep rate at two different stresses. If H_0 is independent of the stress but v is different for the two stresses used, then τ_G can be calculated from these values of H at two different stresses.

These arguments will now be tried on the existing creep data for cold-worked Zircaloy. In order to minimize changes of the creep rates caused by neutron flux spectra and other uncertainties, only Fidleris's data in NRX will be used. The stress and temperature dependencies of the in-reactor creep rate are shown in figs. 6 and 7. The slope of the curve for stress dependency at 300 °C is the inverse of that

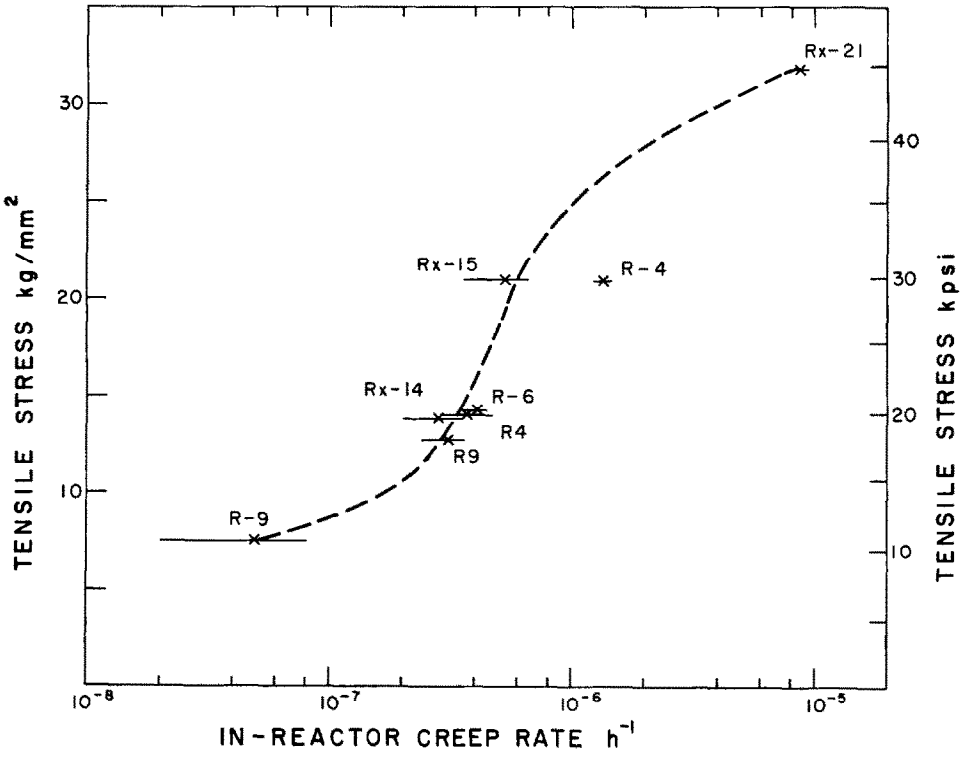

Fig. 6. Stress dependence of the steady in-reactor creep rate of cold-worked Zircaloy at 300 °C [4]) with the creep rates corrected linearly to a flux of 6×10^{12} fast n/cm²·sec.

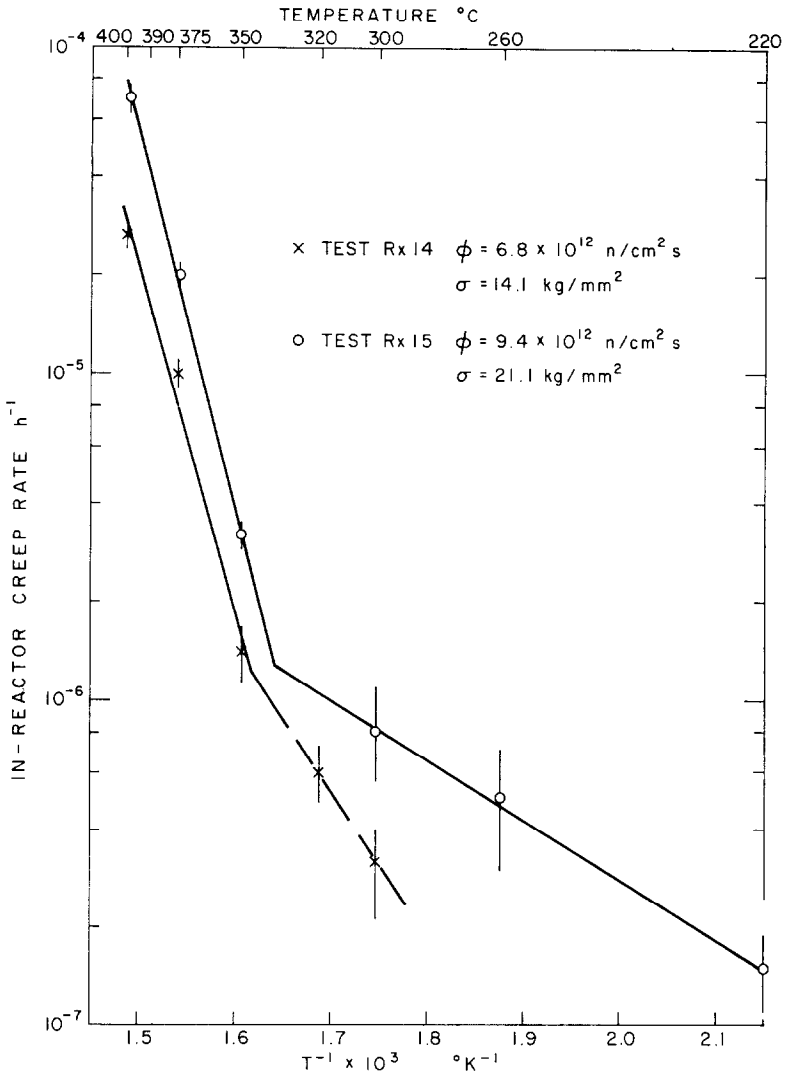

Fig. 7. Temperature dependence of the steady in-reactor creep rate of cold-worked Zircaloy [4]).

given in case (a) above. Therefore, assuming the pre-exponential term varies more slowly than the exponential term, the slope of the curve in fig. 6 is proportional to $1/v$. Obviously, the position assumed for the curve is somewhat arbitrary due to uncertainty in values around 25 kpsi. However, the curve drawn is thought to be the best evaluation and is consistent with the linear stress dependency found in pressure tubes around 18 kpsi (12.7 kg/mm^2). The increase in slope up to about 30 kpsi (21 kg/mm^2) indicates a decrease in activation volume. Above 30 kpsi the activation volume is apparently increasing, which indicates another type of obstacle is beginning to control the in-reactor creep rate. This is consistent with the change from radiation increasing the creep rate for all the stress levels except the highest one shown. At 45 kpsi (32 kg/mm^2) the creep rate was reduced by irradiation. Apparently, the regions of radiation damage must be controlling the creep in this high stress region. The slope of the curve between 20 and 30 kpsi (14–21 kg/mm^2) gives a value of $v = 4b^3$, assuming $r = 0$. Such a low value makes this assumption poor, however. It needs checking when the stress

TABLE H1

Activation energies, H, from in-reactor creep measurements of cold-worked Zircaloy. The value for the shear stress τ, was taken equal to half the tensile stress σ.

Uniaxial tensile stress σ	H(kcal/mole) when $\dot{\varepsilon} < 1 \times 10^{-6}$	$(H_0)_{max} = (H + v\tau)$ kcal/mole	
		$v = 4b^3$	$v = 11b^3$
20 kpsi (14.1 kg/mm^2)	21	22.3	24.6
30 kpsi (21.1 kg/mm^2)	8.4	10.4	13.8

dependency at a different temperature is known. The actual v will be smaller than this if the pre-exponential term, τ^r, carries some of the stress dependency. The activation volume found from a straight line joining the values for tests R9 and Rx-21 in fig. 7 is equal to $11b^3$.

The activation energies found from the slope of the curves below a strain rate of 1×10^{-6}/h in fig. 7 are given in table H1. The maximum values for H_0 calculated for the two different activation volumes given, are also shown in table H1. The large change in H_0 for a stress at 20 and 30 kpsi (14.1 and 21 kg/mm^2) can be caused by two features. Either the effective value of l decreases with increasing stress for one of the reasons previously mentioned, or else the temperature dependence of the mobile dislocation density is higher at the low stress. The mobile dislocation density may increase with temperature if strain-ageing occurs. Ignoring this positive temperature dependence in the pre-exponential factor would produce too large a value for H_0.

References

1) L. J. Chockie, J. J. Holmes and J. C. Tobin, ASTM Special Techn. Publ. no. 341 (1963)
2) V. Fidleris and C. D. Williams, J. Electrochem. Tech. 4 (1966) 258
3) P. A. Ross-Ross and C. E. L. Hunt, J. Nucl. Mat. (this issue, pp. 2–17)
4) V. Fidleris, J. Nucl. Mat. (this issue, pp. 51–76)
5) S. N. Buckley, UKAEA Report AERE-R5262 (1966)
6) R. V. Hesketh, Phil. Mag. 7 (1962) 1417
7) W. S. Blackburn, Phil. Mag. 6 (1961) 503
8) E. F. Sturcken and J. W. Croach, Trans. AIME 227 (1963) 934
9) J. J. Kearns, USAEC Report WAPD-TM-472 (1965)
10) E. F. Ibrahim, Chalk River (Canada) Report AECL-2528 (1965)
11) R. V. Hesketh, J. Nucl. Mat. (this issue, pp. 77–86)
12) F. S. Rossi, M. Castagna, A. Ferro and J. Sebille, SORIN Report (Italy) 87 (1966)
13) R. V. Hesketh, Phil. Mag. 8 (1963) 1321
14) R. V. Hesketh, Phil. Mag. 11 (1965) 917
15) J. J. Holmes, J. A. Williams, D. H. Nyman and J. C. Tobin, ASTM Special Techn. Publ. no. 380 (1964)
16) L. M. Howe, R. W. Gilbert and G. R. Piercy, Appl. Phys. Letters 3 (1965) 125
17) L. M. Howe and W. R. Thomas, J. Nucl. Mat. 2 (1960) 248
18) G. R. Piercy and J. Lori, results to be published
19) B. A. Cheadle and C. E. Ells, Electrochem. Tech. 4 (1966) 329
20) C. R. Cupp, J. Nucl. Mat. 6 (1961) 241
21) J. Worster and N. H. March, J. Phys. Chem. Sol. 24 (1963) 1305
22) J. Lindhard, M. Scharff and H. E. Schiott, Mat. Fys. Medd., Dan. Vid. Selsk 33, no. 14 (1963)
23) G. R. Piercy and R. H. Tuxworth, Chalk River (Canada) Report AECL-1261 (1961)
24) A. J. Ardell, Acta Met. 11 (1963) 591
25) L. M. Howe, to be published
26) C. D. Williams and C. E. Ells, to be published
27) T. D. Gulden and I. M. Bernstein, Phil. Mag. 14 (1966) 1087
28) M. L. Swanson, Can. J. Phys. 44 (1966) 3241
29) G. V. Kidson, Electrochem. Tech. 4 (1966) 193
30) K. Mukherjee, Phil. Mag. 12 (1965) 915
31) J. F. Nye, Physical properties of crystals (Oxford Press, 1960)
32) E. S. Fisher and C. J. Renken, Phys. Rev. 135 (1964) A482
33) R. F. S. Hearmon, Acta Crys. 10 (1957) 121
34) R. E. Reed-Hill, E. P. Dahlberg and W. A. Slippy Jr., Trans. AIME 233 (1965) 1766
35) D. Weinstein, Electrochem. Tech. 4 (1966) 307
36) F. Kroupa, Theory of crystal defects (ed. B. Gruber; Academic Press, 1966) p. 275
37) A. J. E. Foreman, Acta Met. 3 (1955) 322
38) W. Tyson, Acta Met. 15 (1967) 574
39) G. B. Gibbs and J. A. Turnbull, Met. Sci. J. 1 (1967) 25
40) N. F. Mott, Phil. Mag. 44 (1953) 742
41) J. Friedel, Dislocations (Pergamon Press, London, 1964) p. 113
42) D. Rosenthal, Trans. ASME 68 (1946) 849

[43]) C. R. Barrett and W. D. Nix, Acta Met. **13** (1965) 1247
[44]) W. D. Nix, Acta Met. **15** (1967) 1079
[45]) J. J. Holmes, Acta Met. **15** (1967) 570
[46]) G. Schoeck, Mechanical behaviour of materials at elevated temperatures (ed. J. E. Dorn, McGraw Hill, 1961) p. 79
[47]) J. Friedel, Dislocations (Pergamon Press. 1964) p. 405
[48]) F. J. Heinrich, USAEC Report DP-906 (1964)
[49]) H. Conrad, J. Metals **16** (1964) 582
[50]) G. Schoeck, Phys. Stat. Sol. **8** (1965) 499
[51]) A. J. E. Foreman and M. J. Makin, Can. J. Phys. **45** (1966) 511
[52]) T. J. Koppenaal and D. Kuhlmann-Wilsdorf, Appl. Phys. Letters **4** (1964) 59